

Visual-Vestibular Integration as a Function of Adaptation to Space Flight and Return to Earth

(DSO 604 OI-3)

Millard R. Reschke, Jacob J. Bloomberg, Deborah L. Harm, William P. Huebner, Jody M. Krnavek, and William H. Paloski of the Johnson Space Center, Houston, TX; Alan Berthoz of the Laboratoire de Physiologie de la Perception et de L'Action, College de France, Paris

BACKGROUND

Research on perception and control of self-orientation and self-motion addresses interactions between action and perception [1]. Self-orientation and self-motion, and the perception of that orientation and motion are required for and modified by goal-directed action. Detailed Supplementary Objective (DSO) 604 Operational Investigation-3 (OI-3) was designed to investigate the integrated coordination of head and eye movements within a structured environment where perception could modify responses and where response could be compensatory for perception. A full understanding of this coordination required definition of spatial orientation models for the microgravity environment encountered during spaceflight.

The central nervous system (CNS) must develop, maintain, and modify as needed, neural models that may represent three-dimensional Cartesian coordinates for both the self (intrinsic) and the environment (extrinsic). Extrinsic coordinate neural models derive from the observer's ability to detect up/down vector signals produced by gravity (g) and visual scene and polarity (VS). Horizontal coordinates are incompletely specified by the up/down vector. Additional complexity is introduced because extrinsic coordinate models derive from multimodal processes. For example, detection of gravity is mediated by graviceptors at several locations in the body, including the vestibular apparatus (Gves), somatic receptors (Gs), and visceral receptors (Gvic) [2, 3]. Intrinsic coordinate models must be more complex because they may be eye centric, head centric, torso centric, and so on [4]. Intrinsic coordinate models also should differ from those for extrinsic coordinates in that X-, Y-, and Z-axis vectors are all nonarbitrary and physiologically specified [5].

Effective action in the normal environment requires mapping of relationships between models for intrinsic coordinates relative to the model for extrinsic coordinates. The resulting maps may be used in at least two ways: perception of body orientation, and determination (settings) of initial conditions for central motor control command system(s). Eye/head movements during visual target acquisition, limb movements during reaching for targets, and locomotion toward goals all require motor control.

While earlier studies suggested a common (shared) central motor command system, more recent research suggests parallel command pathways, at least for the head and eye during visual target acquisition control [6].

Recent advances in neuroscience suggest that central neural processing involves activity in multiple, parallel pathways, also known as distributed functions or distributed networks [7]. Based on these advances, and the evidence for parallel motor control systems, we postulated multiple, parallel maps relating intrinsic and extrinsic coordinate neural models. These parallel maps may be associated with different processes, including perception of whole body motion, limb target acquisition, and head/eye target acquisition. For effective reaching or locomoting toward a target, the map that provides initial conditions for the limb motor control system would require weighting of the intrinsic Z body axis. For effective looking for a target, the map that provides initial conditions for head/eye motor control would require weighting of the intrinsic Z head and retinal meridian axes.

Self-orientation and self-motion perception derives from a multimodal sensory process that integrates information from the eyes, vestibular apparatus, and somatosensory receptors. Perhaps due to these underlying multimodal processes, self-orientation perception is not referred to any single receptor or body location [8] in the sense that a tactile stimulus is referred to a location on the body surface, or that visual stimuli are referred to the eyes. For example, self-orientation with respect to gravitationally defined vertical can be reported employing numerous procedures such as setting a luminous line, positioning a limb in darkness, or verbally reporting perceived head position in darkness.

Useful reviews of spatial orientation research by Howard and Templeton [9], Guedry [10], and Howard [4, 11] include the following:

1. Observers are able to report perceived orientation with respect to extrinsic reference vectors (axes) defined by gravity, visual scene polarity, and tactile polarity, and to intrinsic reference vectors such as the eye, head, or torso Z axes (Z_e , Z_h , and Z_t , respectively).
2. Reports can be obtained verbally as well as by movements of the eyes, movements of the limbs, manipulation

of a tactile stimulus (rod) and movement of a visual line, and report accuracy can be judged with respect to the reference vectors.

3. Reports indicate a compromise when visual and gravitational reference vectors are not parallel, as in rod and frame studies, and tilted room experiments.

4. Studies show that discrepancies between gravity and internal Z-axis vectors may also influence reports. For example, reported tilt of a truly vertical line in the direction opposite to the head tilt implies that the subjective visual vertical is tilted in the same direction as the head tilt. This A (Aubert) effect predominates when body tilt is large ($> 60^\circ$) [4], and can be understood by relating extrinsic G- and intrinsic Z-axis vectors [12, 13].

5. Observers are able to estimate accurately rotational displacement solely on the basis of semicircular canal cues within known limits of rotational velocity and amplitude [10]. Consequently, whole body rotation can be used in microgravity, analogous to static head tilt on Earth, to produce a disturbance, compensation for which indicates weighting of neural signals that indicate extrinsic VS and intrinsic Zt reference vectors as well as changes in their weighting during microgravity adaptation [14].

Reviews of recent research concerning sensorimotor adaptation in microgravity [15-18] suggest that in the absence of a gravitational reference axis (G), astronauts initially exhibit increased reliance on visual reference axes derived from VS coordinates [15, 19], and that during prolonged microgravity exposure, reliance may shift toward intrinsic reference vectors, including Ze, Zh, Zt [20-22]. Alteration of sensory processing, such as labyrinthectomy, or rearrangement of environmental features, as in prolonged exposure to microgravity, requires adaptation for effective motor control. One aspect of adaptation may involve re-mapping of intrinsic and extrinsic coordinate relationships. In the normal adapted state, parallel maps are likely to be congruent. During adaptation, these maps may differ and adaptation may be complete when the parallel maps are once again congruent.

Perceptual and oculomotor response discrepancies, observed during adaptation to stimulus rearrangements, support these concepts. Except in the case of ocular torsion and perceived tilt [23], perceptual and oculomotor responses are normally approximately congruent [10]. However, response incongruence has been noted during adaptation to unilateral loss of vestibular function when the spinning sensation gradually subsides, while peripheral asymmetry, as revealed by eye movement records, remains [24]. Similar response incongruence has been observed following exposure to stimulus rearrangements, including the inertial visual stimulus rearrangement produced by microgravity.

Perhaps the most dramatic case of perceptual oculomotor response incongruence was reported by Oman et al. [25]. After 1 to 3 hours of wearing goggles that

produced a left-right reversal of the visual field, subjects exposed to a moving stripe display reported illusory self rotation in the same direction as the observed stripe motion. However, no subject showed evidence of reversal of the VOR slow phase component. More recently Oman and Balkwell [26] reported that during microgravity, a nystagmus dumping procedure consisting of a 90° forward head pitch following a sudden stop from $120^\circ/\text{sec}$ rotation, resulted in an almost instantaneous termination of perceived self rotation. However, post-rotatory nystagmus durations were as long as those observed before and after spaceflight when the head was held erect (no dumping). These and related observations led Peterka and Benolken [24] to suggest that the neural mechanisms underlying central compensation may not be fully shared by vestibular reflex and self-motion perception systems. Our suggestion of re-mapping the relationships between intrinsic and extrinsic coordinate neural models appears to be a variation of their hypothesis.

If the fully adapted state is characterized by congruence among parallel maps, one implication is that different re-mapping processes may occur across different time intervals during adaptation. Given that the re-mapping processes suggested here would be a form of sensorimotor learning, that would almost certainly be true. Of the conditions that facilitate sensorimotor learning, active, voluntary motion is among the most important [27]. The rate of re-mapping would be dependent upon the classes of voluntary actions performed. If an observer were to engage only in head/eye target acquisition behaviors, one might expect that the map serving the head/eye motor control system would be altered sooner than would the map serving limb motor control.

The vestibulo-ocular reflex (VOR) serves to maintain a clear image on the retina by producing eye movements that compensate for perturbations of the head. The VOR is mediated by vestibular information relying on appropriate canal-otolith interaction for effective gaze stabilization. On Earth, the direction of the gravity vector sensed by the otoliths is thought not to vary during yaw head oscillations [28]. Several investigations of the effects of microgravity on yaw VOR have been conducted. In-flight experiments have relied on voluntary head oscillations at frequencies ranging from 0.25 to 1 Hz [29-33]. Passive rotation has also been employed before and after spaceflight [33]. Head oscillations were performed with eyes open fixating a wall target where gain was presumably 1.0, and with eyes open in darkness or eyes closed while imagining a wall-fixed target. Few studies have detected significant preflight or postflight changes in yaw VOR [29, 32, 33]. When changes were noted, the direction of the change varied between subjects [34].

In an experiment conducted aboard the U.S. Space Shuttle, a subject who was instructed to use an imaginary wall-fixed target during head oscillations, exhibited decreased VOR gain at 0.25 Hz on his first test six hours

into the mission [31]. VOR recovered to preflight levels by flight day 7. This finding of decreased VOR gain early in microgravity was consistent with the parabolic flight and centrifuge results of others who have demonstrated decreased VOR gain with decreasing gravity [35, 36]. Since no phase shift accompanied the in-flight reduction in VOR, suppression of vestibular input by the subject may have occurred. The subject was trained as a pilot, so suppression to avoid sensory conflict could have been learned. It is also possible that the subject could not imagine a wall-fixed target in the absence of gravity [31].

Parabolic experiments by DiZio and colleagues [37, 38] demonstrated that the apparent time constant of post-rotatory nystagmus (PRN) in yaw and pitch was shortened during, but not after, acute exposure to microgravity. Yaw axis PRN to a step velocity rotation, using a hand-spun rotating chair, was monitored in flight in one crew member on a Shuttle mission. The results indicated no change in gain and were suggestive of a shortened time constant in flight. The nystagmus dumping phenomenon appeared during flight, suggesting that it could be triggered by processes related to the active head movement rather than by gravity *per se* [39].

Comparisons of preflight and postflight PRN among nine Shuttle astronauts have shown a residual shortening of the apparent time constant, but no consistent change in the magnitude of the initial peak slow phase velocity response during the first several days after return from a week-long flight [40, 41]. The effects were thus qualitatively similar to those observed by DiZio et al. [37, 38] in parabolic flight. Responses gradually returned to preflight norms during the first week after landing. Oman et al. [42] have speculated that as a consequence of the altered gravireceptive input in microgravity, the CNS may have reduced the vestibular component driving central velocity storage in favor of visual inputs.

In contrast to yaw, pitch head oscillations in normal gravity produce changes in the direction of the gravity vector sensed by the otoliths. The microgravity environment offers an ideal way to investigate the contribution of the otoliths to pitch VOR [28]. In-flight investigations of pitch VOR have employed voluntary head oscillations at frequencies comparable to those described above for yaw. While in-flight and postflight changes have not been observed in some instances [32], other investigations have noted alterations in the vertical VOR. Two subjects exposed to pitch oscillation at 1 Hz demonstrated significantly increased VOR gain in tests 14 hours after landing, compared to day 5 and 7 during flight [28]. In these experiments, an increased phase lag was present during the in-flight tests. However, the change in vertical VOR gain and phase relationship was not statistically significant due to high dispersion of data.

A decrease in vertical VOR gain for 0.25 Hz pitch oscillations was observed with a subject tested on STS-51G [31]. His gain was diminished for the first four days

in flight, after which the gain slowly returned to preflight levels. The results of both experiments conflicted with the increased VOR gain observed during the zero-gravity portions of parabolic flight aboard the KC-135 for pitch oscillation at 0.25 Hz [43]. Possible explanations for these conflicting results include: (1) learned suppression of vestibular input by the STS-51G subject [31], (2) occurrence of adaptation before in-flight measurements on Spacelab-1 (SL-1), (3) testing at a frequency (1 Hz) for which the canals were dominant, or (4) the potential difficulty in imagining a wall-fixed target during spaceflight in the same manner as on Earth [28].

It is hypothesized, based on the work of Guedry [44, 45], Benson and Bodin [46], and Bodin [47] that the differences anticipated between the horizontal and vertical canals are based on differing organizations of the compensatory responses to angular motion about the yaw (Z) axis when compared to the responses in pitch (Y) and roll (X) axes. In the normal upright position, motion in yaw occurs typically without any major changes in the direction of the gravity vector. During oscillation in the other two axes, there is concordant information supplied to the CNS by the vertical canals and otoliths. In a microgravity environment, the canals continue to supply input about the direction and magnitude of rotation while the otoliths, depending on their resting sensitivity level, will not provide the expected information, leading to alteration in VOR function.

Gaze is the direction of the visual axis with respect to space. It is defined as the sum of eye positions with respect to the head, and head position with respect to space. Coordinated eye-head movements toward an offset visual target usually consist of a combined saccadic eye and VOR response that shifts gaze onto target. It has been previously demonstrated that exposure to microgravity of spaceflight induces modification in eye-head coordination during target acquisition [48, 49] and ocular saccadic performance [50]. To achieve this sensorimotor transformation, current models of eye-head coordination postulate that a vestibular signal, specifying head movement relative to space, serves as an integral component underlying saccadic spatial programming during head-free gaze shifts [51, 52]. In these models, desired gaze position is compared to an internal representation of actual gaze position. Actual gaze position is derived by summing an efferent copy of eye position in the head with a vestibularly derived reconstruction of current head position. The difference between desired and actual gaze position produces a gaze position error signal that drives saccadic motor output until the error signal is nullified and eye movement stops.

Recent studies support these models by demonstrating that saccadic eye movements generated in total darkness successfully acquire a just-seen Earth-fixed target after cessation of head angular [53, 54] and linear displacement [55]. Such saccadic eye movements are spatially targeted using remembered semicircular and

otolithic vestibular information. The demonstration of this capability indicates that a functionally meaningful vestibular signal has access to the saccade generating mechanism and may, therefore, play a pivotal role in eye-head gaze shifts.

Given these documented disruptions that occur in VOR function during spaceflight and the putative vestibular coding underlying saccadic spatial coding, the first goal of this study was to investigate components of the eye and head target acquisition system during and following adaptation to microgravity.

Using a special oculomotor mechanism located within the brain, it is possible to fixate the eyes on a small object of interest that is moving relative to a fixed background and follow it voluntarily, without moving the head (smooth pursuit response). This mechanism is primarily driven by differences between the velocity of the object (target) and the instantaneous eye velocity. However, we normally track moving objects of interest with a combination of eye and head movements to keep the object near the center of our field of view and our eyes centered within the skull's orbit. When we rotate our head to track a target, a different reflexive mechanism, driven by the signals initiated within the vestibular system, called the vestibulo-ocular reflex (VOR), acts to counter-rotate the eyes in an attempt to keep unchanged the gaze position, defined as the position of the eye with respect to space. In order to track the moving target during a concurrent head motion, the eye movement command signal from the VOR must in some way be nulled to allow gaze position to change with target position. Studies have shown that the primary signal responsible for cancellation of the VOR during eye-head tracking originates within the smooth pursuit system [56-58], although other signals may also contribute [59-61], and the internal gain of the VOR may be somewhat attenuated [58, 62]. The saccadic system provides a mechanism, anatomically represented by the foveal portion of the retina, that rapidly corrects for gaze position errors by coding ballistic eye movement commands based upon perceived position differences between the target and the center of focus. These saccadic eye movements can be used to correct gaze for limitations in the ability of the smooth pursuit system to provide sufficient eye movement command signals to cancel the command signals from the VOR.

In results reported by Russian investigators [63], changes in pursuit tracking of vertical pulsed movements of a point stimulus were manifested early in flight, on days 3 and 5, by decreased eye movement amplitude (under-shooting) and the appearance of correction saccades. Also during flight, pursuit of a vertically or diagonally moving point stimulus deteriorated while associated saccadic movements were unchanged. The effects of microgravity on the pursuit function were most pronounced early in flight on day 3, after long exposure to microgravity on flight days 50, 116, and 164, and also after flight. Pursuit

was found to be improved following in-flight execution of active head movements, indicating that the deficiencies in pursuit function noted in microgravity may have been of central origin [63]. Further analyses of these data indicate that, although postflight tracking seemed to provide gaze changes comparable to target motion, the relative contributions of saccades and smooth pursuit eye movements to the overall gaze changed relative to preflight values. Postflight gaze relied much more heavily upon saccadic contributions, generated due to position errors, that were both more frequent and of larger amplitude. Also, slow phase eye velocity was actually in the opposite direction of head motion, indicating that the VOR was incompletely canceled by the smooth pursuit system. The latter suggests that adaptation to spaceflight caused either an appreciable change in the gain of the VOR, a reduction in the efficacy of the smooth pursuit system, or both.

In contrast, tests of two cosmonauts in the Mir Station, during the ARAGATZ mission, showed that horizontal and vertical smooth pursuit were unchanged in flight [64]. However, results of corresponding saccadic tasks showed: (1) a tendency toward over-shooting of a horizontal target early in flight with high accuracy later in flight, (2) increased saccade velocity, and (3) a trend toward decreased saccade latency.

The stability of the visual world during voluntary eye and head movements depends upon a complex physiological integration of stimuli and perception that is interrupted by the brain in response to changes in the inertial environment. Performance of the ocular motor system undergoes constant recalibration and adjustment to assure optimal visual capability during adaptation to microgravity and subsequent return to Earth. Adaptation of vestibulo-ocular motor motility in one inertial environment is not appropriate for proper physiological function in another inertial environment. Further, erroneous perception of self-motion or surround motion drives compensatory eye movements that are inappropriate for the new inertial environment. This leads to an additional degradation of sensory-motor function.

Physiological failure of eye movement is best defined by considering function. The vestibular, optokinetic, and visual fixation systems act to hold images of the seen world steady on the retinal fovea. Their function is to hold gaze steady. Saccades, smooth pursuit, and vergence work together to acquire and hold objects of interest on the fovea. Their function is to shift gaze. DSO 604 OI-3 was designed to investigate the ability of spaceflight crew members to perform both of these functions. Specifically, physiologic failure of eye movement function occurs during and immediately following a gravito-inertial transition, such as exposure to microgravity and return to Earth. At such times the ability to perform one or more of the following functions has been compromised: (1) hold an image on the retina when the head is stationary, (2) hold an image on the retina during brief head movements, (3)

hold an image on the retina during sustained rotation of self or surround, (4) hold the image of a moving target on the retina, (5) bring images of objects of interest onto the fovea, or (6) maintain accurate perceptions of self-motion and surround motion. The final common pathway of dysfunction in all of these responses is failure to acquire and/or maintain an image of interest on the fovea.

A vestibulo-ocular sensory-motor system that is inappropriately adapted for the inertial environment can result in errors during spaceflight activities, including errors in spatial orientation, delays in visually capturing operationally relevant targets, switch throws, satellite capture, object location, or manipulation of objects. During reentry, errors can occur in acquiring information from instrumentation, switch throws, eye/head/hand coordination, attitude control, perception of altitude, pursuit of an object that is either moving or stationary relative to the crew member, or delays in pursuit and capture of visual, tactile, or auditory targets. Errors during nominal egress activity may include difficulty with visual target acquisition, pursuit of a moving object, or inappropriate perceptions that can result in inappropriate head stabilization strategies, which in turn can affect postural stability and locomotion. Errors during emergency egress may cause problems that could result in personal injury.

Risk of operational failure is hypothesized to be related to: (1) flight duration—the longer the flight the higher the risk, (2) smoke, darkness, crew complement, and circumstances where the Shuttle is in an unusual attitude, and (3) prior spaceflight experience. Risk is the end product of inappropriate response patterns leading to failure in an operational setting. Eye movements must be accurate and precise or the crew member will become susceptible (i.e., at risk) to the dangers of the flight environment. Greater risk is associated with environments that require constant vigilance, timely responses, and accurate visual target identification and/or location. Therefore, risk is defined in terms of the ability of the crew members to correctly perceive their orientation in three-dimensional space. Specifically, orientation is considered to involve the correct determination of the dynamic position and attitude of self or spacecraft in three-dimensional space. The key word here is “dynamic,” implying full knowledge of self-motion, or motion of the spacecraft, as well as the static position of instruments and a geographical point of reference.

Crew member loss of veridical orientation is operationally defined as spatial disorientation. For convenience, and consistency of nomenclature designators of spatial disorientation in the spaceflight environment, spatial disorientations are assigned to one of two categories. Spatial disorientations in the Type I category refer to loss of orientation without the knowledge of the crew member. In this case crew members fail to sense correctly their position in space, may improperly locate instrumentation and geographical references, and then may act on erroneous perceptions. In the Type II disorientation category, crew

members recognize that they are disoriented and can resolve the sensory conflict. It is important to recognize that it is possible, indeed highly likely, that spatial disorientation can and does occur without the knowledge of either the pilot/commander or other members of the crew. Even when crew members are entirely cognizant of the immediate consequence of their spatial disorientation, and recognize that with head movements vision is blurred or that they have thrown an incorrect switch, it is frequently assigned less importance than it merits, and the importance declines with distance from the incident. In part, avoidance of spatial disorientation requires accurate and timely foveation of visual targets. Anatomical, physiological, and physical parameters define the minimal criteria for performance that will maximize foveation and veridical perception of true spatial orientation.

Anatomically, the fovea of the eye has variously been reported to subtend a visual angle ranging from $\pm 0.25^\circ$ to $\pm 4.0^\circ$, depending on the author or measurement technique. However, it is clear that a linear function (as described psychophysically) shows that by the time gaze has deviated by as little as 1.0° from absolute foveal center, visual acuity falls off by a factor of two to three. Therefore, clear unambiguous perception requires that the selected target be maintained within approximately $\pm 0.5^\circ$ relative to central foveal gaze. Physiologically, time to foveate a target depends upon the command process issued for target acquisition. Typically, only about one ten-thousandth of our visual field is clearly seen, but we are not at a loss because our eyes continually move (small saccades) to point the area of the central fovea toward the object of interest. However, physiologically, the cost of the small corrective saccades is approximately 200 msec/saccade. Physically, target acquisition depends upon the location (distance and direction the head and eye must be rotated to foveate the target) and the type (spatial frequency) of the target.

A number of investigators have assessed the role of vestibular-based subsystems both during and immediately following exposure to microgravity [17, 18, 65]. While these assessments provide information specific to one or more sensorimotor subsystems, there is little documentation of changes in the strategies used for coordination among subsystems or for those strategies supporting performance of natural, goal-directed behaviors. Among the several strategies selected for use during the process of adaptation to microgravity are: (1) reduced use of head movements during early phases of the mission, (2) reliance on either an internal coordinate system (intrinsic) or environmental coordinates (extrinsic) during different phases of space flight for spatial orientation, and (3) compensation for the changing role of proprioceptive information during flight. Strategies developed during spaceflight are transferred to behavior immediately following a return from orbit. The newly acquired behavior is not appropriate, and responses, particularly in off-nominal situations, will result

in performance decrements. These strategies can be evaluated using goal-directed head and eye coordination tasks. Therefore, the primary objective of this study was to investigate the emergence or alteration of goal-oriented strategies required to maintain effective gaze when the interactive sensorimotor systems required for this function were modified following exposure to the stimulus rearrangement of spaceflight, and to relate changes in the newly developed strategy to changes in parameters that would degrade performance.

METHODS

A number of experiment paradigms classified as voluntary head movements (VHMs) were selected and designed to investigate changes in spatial orientation and strategies as a function of exposure to the stimulus rearrangement encountered during spaceflight. The primary protocols of DSO 604 OI-3 included target acquisition, gaze stabilization, pursuit tracking, and sinusoidal head oscillations. In all cases, participating crew members completed, as a minimum, each protocol three times before flight and three times after flight. When OI-3 was performed in flight, an additional two sessions were required before flight so that protocols could be practiced and data collected within the training mockups of the Shuttle middeck. When collected in flight, data were obtained at least twice—less than 48 hours after launch, and approximately 24 hours before landing. Additionally, data were collected to measure gaze stabilization during entry, starting at Shuttle entry interface minus 5 minutes, and immediately following wheels stop, before seat egress.

The astronauts who volunteered to participate in each of the protocols were provided with informed consent agreements, given a briefing on the intent and purposes of each protocol, and were free to withdraw from the study at any time. All subjects had completed a recent Air Force Class II physical examination, were free from any central nervous system problems, and had normal vestibular function. For those with visual correction, all protocols were completed with the correction in place. The number of subjects participating in each of the three OI-3 protocols are listed in Table 5.3-1 by flight.

Target Acquisition

Acquisition targets were permanently fixed to a tangent screen at predictable angular distances in both the horizontal ($\pm 20^\circ$, $\pm 30^\circ$, and $\pm 60^\circ/68^\circ$) and vertical ($\pm 15^\circ$, $\pm 20^\circ$, and approximately $\pm 55^\circ$) planes (Figure 5.3-1). To easily differentiate between targets, each was color coded ($\pm 20^\circ$ green, $\pm 30^\circ$ red, etc.), corresponding to the degree of angular offset from center.

Table 5.3-1. Operational investigations (OI) performed on designated flights and total number of subjects

Mission	OI-3a	OI-3b	OI-3c
STS-43		1	
STS-44	1		
STS-49		1	
STS-52		2	
STS-53		1	
STS-54	1		
STS-57		2	
STS-51	1		
STS-58		1	
STS-61		3	
STS-62		4	
STS-59		2	
STS-65		1	1
STS-68			2
STS-64		3	
STS-66		2	
STS-67			3
STS-69		3	
STS-73			2
STS-72			2
<i>Totals</i>			
20	3	26	10

OI-3a - Preflight, In-flight, Entry, Wheels Stop, Postflight

OI-3b - Preflight, Postflight

OI-3c - Preflight, In-flight, Postflight

For all target acquisition tasks, the subject, using a time optimal strategy, was required to look from the central fixation point to a specified target indicated by the operator as quickly and accurately as possible, using both the head and eyes to acquire the target. Each of the 12 targets was acquired a minimum of two times. When target acquisition was performed during flight, measurements were obtained using a cruciform target display on the mid-deck lockers. In all cases eye movements were obtained with both horizontal and vertical electro-oculogram (EOG). Head movements were detected with a triaxial rate sensor system mounted on goggles that could be fixed firmly to the head. Both the head (using a head-mounted laser) and eye movements were calibrated using the color coded acquisition targets.

Gaze Stabilization

Ocular stabilization of a stationary target, during active yaw and pitch head movements, was investigated using a gaze stabilization paradigm with the following steps: (1) the subject visually fixated a wall-fixed target with head in a central position, (2) when the goggles became opaque and vision occluded, the subject rotated

the head while maintaining pursuit. When the gaze seen wall-fixed target, (3) when the goggles became clear, the subject refixated the target, if necessary, with eyes only, and (4) the head was rotated back to center, keeping eyes on the target. During testing before and after spaceflight, and during flight, subjects performed a minimum of six trials in ya
pitc

stabilization protocol was performed during entry, horizontal and vertical trials were alternated. A single fixation point was affixed to the Shuttle forward middeck lockers, directly in front of the subject at a neutral gaze position. The trials began at the Shuttle entry interface and continued nonstop until 5 minutes had elapsed or the Shuttle had landed. Following Shuttle roll-out (wheels stop), the gaze stabilization trials, patterned after those accomplished during entry, were performed for 5 minutes. The entry and wheels stop protocols were difficult because the head movements were performed inside of the helmet, using special goggle devices to assist in recording head and eye movements. As expected, the helmet restricted head movement amplitude.

Pursuit Tracking

Pursuit tracking studies, designed to measure the effectiveness of both smooth pursuit eye movements and combined eye-head tracking in acquiring and maintaining gaze on a moving target, were conducted before and after flight. All trials required the crew member to track the apparent smooth movement of a laser projected on a blank neutral gray tangent screen, first with just the eyes (smooth pursuit), and subsequently using eye movements in concert with active, self-generated head movements (combined eye-head tracking). The subject was positioned 86 cm from, and facing, the tangent screen. Two types of target motion trials, unpredictable and predictable, were presented for each plane of motion.

For stimuli requiring unpredictable target tracking, the target was initially stationary in the center of the field of view (Figure 5.3-2). At an unpredictable time, the target began to move at constant velocity, either to the right, left, up, or down [66] as determined by a schedule of systematic randomization. The target traveled at either 15°/sec or 30°/sec, through a minimum displacement of 30° horizontally or 20° vertically. The onset time of target motion, direction of motion, target velocity, and final target displacement were randomized to eliminate the possible effects of predictive mechanisms, known to affect pursuit tracking responses [67, 68].

In trials involving predictable target motion, the target initially moved horizontally with respect to the subject, then repeated using vertical target motion (Figure 5.3-3). The target oscillated sinusoidally at two separate and individual frequencies at rates that held peak velocity essentially constant at approximately 63°/sec. The frequencies

were 0.333 Hz through $\pm 30^\circ$ horizontally and $\pm 20^\circ$ vertically, and 1.4 Hz through $\pm 7.14^\circ$ horizontally and vertically. Each trial of sinusoidal tracking was performed twice with a minimum of 6 cycles per trial.

Sinusoidal Head Oscillations (Head Shakes)

To perform this test, the subject was first positioned with the wall-fixed target located at the center of the visual field. The subject then attempted to maintain visual fixation on the target while smoothly oscillating the head in either the horizontal or vertical plane, in cadence with an audio tone (1-2k Hz) that was sinusoidally modulated at each of either three or four frequencies (0.2, 0.3, 0.8, and 2.0 Hz). Angular displacement of head oscillation was selected by the subject. Following a collection of responses to a minimum of 10 cycles at each frequency, the visual field was occluded by activating the Electronic Light Occlusion Goggles (ELOGs) with a control voltage, making them opaque. Immediately upon occlusion of the visual field, the subject repeated head movements at each of the individual frequencies while attempting to maintain visual fixation on the remembered target. Subjects repeated this entire procedure in each plane for each visual condition twice for a total of three trials. Special attention was paid to cross-axes head movements, corresponding compensatory eye movements, and changes in head movement control.

Calibration of Head Position in Space

Head position measurements were calibrated by activating a low power laser mounted on the browpiece of the plastic web cap firmly affixed to the subject's head. The cap and laser were adjusted so that the laser was located centrally on the forehead, between the eyes. With the subject's head in the zero or neutral position, the laser was adjusted within a swivel mount to align with the 0° target. Visual feedback from the laser allowed the subject to accurately align the head with a given calibration target. Movements were made successively between the central target and each calibration target in both the horizontal and vertical planes. At least two trials to all targets were performed at the beginning of each experiment, and repeated if for any reason the plastic web cap had been disturbed or removed.

Measurement of Head Position

Active head movements were measured using a triaxial rate sensor bundle integrated on the same plastic web cap that housed the positioning laser. The rate sensor was located approximately on the apex of the skull, and adjusted prior to each test session, to minimize cross talk between the yaw, pitch, and roll axes. Software was developed to remove any residual cross talk. Three rate sensors separately transduced yaw, pitch, and roll head velocity movements. From these sensors, horizontal (yaw), vertical

(pitch), and roll head position wave forms were obtained using digital integration techniques, following initial processing performed to remove any offset signal in the rate sensors.

Occlusion of Vision

Because the corneo-retinal potential changes with drastic shifts in illumination and effects EOG measurements, special Electronic Light Occlusion Goggles (ELOGs) were developed, using a polymer dispersed liquid crystal or PDLC. In its normal state, the PDLC was opaque and transmitted up to 98% of the light, much like frosted glass. When an appropriate voltage was applied across this plastic, it became transparent. Transformation from opaque to visible was virtually instantaneous, did not significantly change the relative illumination level to the subject, or alter the measured EOG gains. When vision was occluded with the ELOGs, the visual “scene” was featureless and provided no fixed visual reference.

Eye Movement Measurement and Calibration

Eye positions were measured during all phases of the test, using standard electro-oculography. Disposable infant non-polarizing ECG electrodes were applied to the outer canthus of each eye to measure horizontal eye movements. Vertical electrodes were applied above and below the right eye, equally distant from the pupil during straight ahead gaze, to capture vertical eye movements. A ground electrode was applied to a neutral surface behind the right ear. During flight, signals were amplified with a gain of 4000 and recorded on tape. Before and after flight, signals were directly digitized with a sampling rate of 500 Hz. To remove extraneous high frequency noise, the measured wave forms were digitally filtered before processing with a finite impulse response (FIR) low pass Hamming window filter, with a nominal cutoff frequency [-3 decibel (dB) point] of 30 Hz. Data were passed through the filter twice, once forward in time and once backward in time, to eliminate all phase shifts and double the stop-band attenuation.

Eye movements were calibrated with a tangent screen before and after flight, and with a locker-mounted cruciform target display in flight. The subject was instructed to acquire the target with rapid eye movements and the head held stationary, from the central target (0°) to the $\pm 20^\circ$, $\pm 30^\circ$ targets in the horizontal plane, and to the $\pm 15^\circ$, $\pm 20^\circ$, $\pm 30^\circ$ targets in the vertical plane. At least two trials to all targets were performed at specific intervals during the experiment, to allow characterization of possible variations in EOG eye movement gain.

Because of the well-known drawbacks of using standard EOG, two novel processing techniques were used: (1) a method for determining and constraining a piecewise quadratic curve derived from the nonlinear response

characteristics of vertical EOG, allowing quantitative calibration of the vertical EOG, and (2) an alternate, dynamic technique for generating horizontal and vertical EOG calibration curves by measuring the EOG signals generated when the eyes move to maintain fixation on a stationary target, while the subject slowly oscillates the head in either the horizontal or vertical plane.

Eye Calibration Using Multiple Fixed Targets

Vertical EOG (Figure 5.3-4a), unlike horizontal EOG (Figure 5.3-4b), is characterized by the volts-to-degrees relationships being generally nonlinear, showing dramatically different voltage outputs for identical upward and downward eye movements. In previous attempts to model this relationship, different investigators have used functions such as third order polynomials or piecewise linear curves joined at zero. Both of these functions may introduce large calibration errors because they are either under (cubic) or over (piecewise linear) constrained. The optimization of function and fit was empirically determined by measuring eye movement responses between zero and multiple targets along the vertical axis spanning the oculomotor range necessary to characterize the data obtained for this DSO. The best approximation to the measured volts-to-degrees relationship came from using a piecewise quadratic function, joined at zero degrees, but not constrained to be zero volts there, and having a continuous first derivative through the connection. This curve matched DSO data through the entire oculomotor range, and essentially the same curves were obtained when calculated using only those targets available to the DSO protocol. As expected, the piecewise linear curve did a satisfactory job of characterizing the data midway between the upper and lower ranges, at the expense of errors near zero and at the oculomotor extremes. The cubic curves usually did a satisfactory job of modeling the dense data. However, when the more sparse data sets were used for calculation, the curves were occasionally less “well-behaved” at the ends of the range and could not be used.

Figure 5.3-5 summarizes the effects of using piecewise linear, piecewise quadratic, and piecewise quadratic with continuous first derivative vertical eye calibration curves on a crew member’s target acquisition trial of combined head and eye movements used to acquire a stationary eccentric target. As can be predicted from the corresponding calibration curves, the piecewise linear curve (Figure 5.3-5a) caused the eye movement response to undershoot for low displacements and to overshoot for higher amplitude displacements. Thus, although a piecewise linear structure for the vertical EOG calibration curve accounted for vertical calibration asymmetries, it provided an unrealistic calibration mapping for the data, resulting in considerable differences (errors) in the calculated response wave forms. To obtain a better fit for the calibration segments, the calibration components were

allowed to assume second order curve characteristics (quadratic). As can be seen from Figure 5.3-5b, this technique was better equipped to accurately map the conversion from measured volts to displayed degrees. However, this piecewise continuous curve near zero had a considerable discontinuity in slope, with the negative displacements approaching zero almost linearly while the small positive displacements rapidly “bulged” in displacement for small changes in input voltage above zero. This rapid change in slope was not characteristic of a physiological system in which changes in calibration mapping, due to system nonlinearity, are probably more gradual. For this reason, we constrained the piecewise quadratic curves to have a continuous first derivative (Figure 5.3-5c). As expected, the differences due to these latter two techniques were small except at low displacements where the response from the curve with unconstrained slopes at zero caused a slight increase in displayed displacement. It is for this reason that we scaled all of our vertical EOG data using piecewise quadratic calibration curves with continuous first derivatives at zero.

Eye Calibration Using Fixed Target and Head Movements

An alternate, dynamic technique for generating horizontal and vertical EOG calibration curves was developed. This technique measured the EOG signals generated when eyes were moved to maintain fixation on a stationary target while the subjects slowly oscillated their heads in either the horizontal or vertical plane. As the head rotated through a certain angle, the eyes generally counter-rotated back through the same, but opposite, angle to maintain fixation. Based on this relationship, angular head position was used to determine the expected eye position required to maintain fixation. These expected eye positions were compared with the corresponding measured EOG voltages to yield the volts-to-degrees relationship necessary for calculating a calibration curve (Figure 5.3-6). Satisfactory fits of the calibration data were obtained from cubic polynomials, although we chose to fit the data with polynomials of lower orders when possible. There were two main advantages of using this dynamic calibration technique:

1. A calibration curve was constructed from hundreds, or even thousands, of data points, whereas calibration curves determined from static calibration data normally were based on 20 points or less.
2. Because each subject individually controlled the peak amplitude of head oscillation, a curve was generated to span each subject’s complete oculomotor range. In this way, subjects were not required to view targets outside of their oculomotor range or to view targets that did not reach the limits of their oculomotor range. This is particularly important because it is at the extremes of the oculomotor range that the largest EOG nonlinearities occur in the vertical plane.

EOG Signal Drift

Aside from the nonlinearity of the vertical EOG, another drawback to using EOG was the problem associated with signal drift. Processing software was developed to optimally and simultaneously scale wave forms (calibration trials) and remove drift. This method was based on a “pseudo-inverse” least squares technique, in which the drift over a trial segment was modeled as an arbitrary order, first order default polynomial. A set of polynomial coefficients and a constant wave form scale factor were calculated, over response regions selected by the operator, to optimally match the measured eye position wave form with the expected eye position wave form that was calculated from the known target and measured head positions. This method was much more robust and reliable than techniques that either ignored the drift or separately calculated the underlying drift characteristics and the calibration scale factor.

Head and Eye Geometry Effects

The geometric effects that the eccentric position of the eyes in the head had on the processing of our target-directed eye and head movement data were considered. Although many laboratories have facilities that allow “far” target viewing, in which geometric considerations have little consequence, space constraints have forced the visual targets to be close to the subject, so that the eccentric position of the eye in the head may no longer be considered negligible. Tests of astronauts on the Shuttle were conducted with extreme spatial constraints, the nominal distance from subject to target display surface being 86 cm.

Oculomotor researchers have historically calculated gaze (the angle of the eye with respect to space) as the simple sum of eye and head wave forms. However, because the axes of head rotation and eye rotation are different, and because the subject was closer than optical infinity relative to the targets, the relative locations of these rotational axes, as well as the magnitude of the rotation about the axes, were considered when interpreting gaze values. This was further complicated because the axis from which target positions were specified did not coincide with either the head or eye rotation axes. Several investigators have demonstrated the dangers of assuming that visual targets lie at optical infinity, and they note the importance of considering the eccentric position of the eyes in the head [58, 69-74]. Clearly, gaze displacement and target displacement were not equal, even if the subject maintained fixation on the target, due to eye eccentricity.

Two basic approaches to analyzing data were used to deal with this geometry issue. The first technique involved comparing measured eye movements with expected eye movements, while considering the geometric relationships between the eye, head, and target. This approach allowed for the direct evaluation of oculomotor performance without modifying the measured eye or head wave forms by

calculating the position of the target with respect to the eye, no matter where the eye was in its plane of motion. This same calculation also provided for the spatial relationships between the eye and head, and between the head and target. The second approach involved adjusting the measured eye movement data to compensate for different axes of head and eye rotation [58]. This technique standardized the measured eye (gaze) position data by mathematically relocating the apparent eye position to the center of head rotation. In this way, eye eccentricity effects were eliminated. This approach provided more data analysis flexibility. Direct comparisons of response wave forms were made from multiple trials, both within and between subjects, by inherently accounting for trial-to-trial variations in head or target motion. Both techniques were used to analyze active eye and head movement data.

The information in Figure 5.3-7 demonstrates that when the head was required to rotate during a trial, it was important to consider the location of the eye in the head when processing eye and head movement data. A trial of Gaze Stabilization is depicted in Figure 5.3-7. The subject fixated a centrally located target. When vision was occluded, the subject rotated the head a comfortable but significant amount while attempting to maintain fixation on the stationary target. When vision was regained, the subject generated a refixation saccade to reacquire the target. Because eye movements were recorded using EOG, a cyclopean eye geometry was assumed, and it was appropriate for the eye to be at zero while fixating a zero target with the head at zero. The panel on the left (Figure 5.3-7a) shows gaze calculated as the simple sum of measured eye and head rotations. The refixation saccade took gaze off target rather than back on target as expected, because gaze was calculated and referenced with respect to the location of the eye in space. Because the rightward rotation moved the cyclopean eye rightward in space, it was appropriate for gaze to deviate leftward to reacquire the stationary target. However, this sort of analysis was not particularly intuitive, and the amplitude of the calculated gaze displacement depended upon the amplitude of the corresponding head movement. To facilitate analysis and interpretation and to remove the effects of eye eccentricity, the geometry considerations to calculate gaze were used as though the measurement was from the location of the cyclopean eye, with the head at zero (Figure 5.3-7b). In this example, gaze drifted off target during vision-occluded head rotation. When vision was again restored, gaze reassumed the expected position at zero. This technique was routinely used to standardize measured signals so that data collected from different subjects or under different conditions could be directly compared.

Verbal Responses

Following each experiment trial, crew members were asked to provide verbal quantitative descriptions of

perceived self-motion and/or visual surround motion, or changes in orientation/position. Primarily, they were asked to specify distinct differences between preflight, in-flight, and postflight sensations. Specifically, they were asked to describe the perceived amplitude and rate of the rotational and/or translational components of self/surround motion following head movements.

RESULTS AND DISCUSSION

Sinusoidal Pursuit Tracking

Sinusoidal pursuit tracking data were used to ascertain the relationships between at least three distinct, functional eye movement systems, as well as how the effects of spaceflight changed these relationships. Neural commands drive eye movements to either: (1) rapidly redirect the line of sight (gaze) to different objects within, or outside of, the field of view, using the saccadic system, (2) track targets moving smoothly relative to the person, such as when tracking the “Ball-Bar” navigation system during entry, using the smooth pursuit system, or (3) maintain gaze on stationary objects of interest, such as cockpit switches, despite head motions, using the VOR. These three systems work together in an attempt to provide the appropriate eye movement command signals to allow the maintenance of fixation on targets despite head or target motion. To tease out the relative contributions from each of these ocular motor systems, we considered the differences in their origins. Table 5.3-2 summarizes which of the fundamental eye movement systems can be expected to contribute to a given test wave form collected in response to a given tracking task.

The saccadic system responds to retinal position errors and is the only fundamental eye movement system that relies primarily on position information. Thus, to determine the contribution to overall gaze from the saccadic system, gaze position errors were compared with gaze velocity errors. If gaze position errors were minimal, but gaze errors were substantially greater when represented in velocity, we concluded that the saccadic system was playing a major

Table 5.3-2. Types of eye movements required for pursuit tracking

<i>Tracking Task</i>	<i>Test Waveform</i>	<i>Component Systems</i>
Smooth Pursuit	Gaze Position	SP, Sacc
Smooth Pursuit	Gaze Velocity	SP
Eye-Head Tracking	Gaze Position	SP, VOR, Sacc
Eye-Head Tracking	Gaze Velocity	SP, VOR

SP = Smooth Pursuit System, Sacc = Saccadic System, VOR = Vestibulo-ocular Reflex

role in supplementing the other eye movement systems to keep the eyes directed toward the target. On the other hand, the smooth pursuit system responds to retinal velocity errors. As long as the head was stationary, we could evaluate the efficacy of the smooth pursuit system by comparing gaze velocity with target velocity. Differences (errors) were attributed to reduced performance of the smooth pursuit system.

Performance of the vestibulo-ocular reflex can be evaluated by inference, through its interaction with the smooth pursuit system during eye-head tracking. During sinusoidal eye-head tracking, the subject tracks a sinusoidally moving target with both the head and eyes, rather than with the eyes alone as during smooth pursuit. Because the VOR responds to head motion and is responsible for maintaining fixed gaze despite head motion, the ability to track moving targets with combinations of eye and head movements requires that the reflexive command signals from the VOR in some way be canceled or suppressed to allow gaze to change along with the target. For cases of eye-head tracking, the VOR is actually an unwanted neurological command signal that must be overcome. Although several possible mechanisms exist to overcome the VOR command signal during eye-head tracking, it is believed that under normal conditions a major contribution to VOR cancellation is the command signal from the smooth pursuit system. Thus, gaze errors observed during eye-head tracking may be due to incomplete cancellation of the VOR by the smooth pursuit system, which could result from (1) reduced efficacy of the smooth pursuit system in providing the necessary cancellation signal, (2) increased VOR gain to a level beyond which a normal smooth pursuit cancellation signal can operate, or (3) some combination of the two.

To assess the effects of spaceflight on the interactions of these three ocular motor subsystems, crew member tracking responses were compared before and after spaceflight. To facilitate comparison of the measured responses, the global gain and phase characteristics of measured gaze responses and their separate eye and head components were calculated relative to their corresponding sinusoidal target counterparts. A gain of 1.0 and a phase of 0.0 indicated ideal overall tracking performance, while deviations from these values indicated changes in performance or tracking strategy. Gain and phase values were calculated for gaze position and velocity wave forms, collected in response to both sinusoidal smooth pursuit and combined eye-head tracking tasks, and for target motion in both the horizontal and vertical planes.

Smooth Pursuit – Saccades and Gaze Error

Figure 5.3-8 shows a typical example of smooth pursuit tracking recorded across subjects when the trial called for pursuing the small laser dot in the horizontal plane at a frequency of 0.33 Hz. Of interest is the change in eye amplitude and the increased number and amplitude of

saccades. The panel on the left shows smooth pursuit approximately 10 days prior to spaceflight. The eye, head, and target are represented by the red, green, and blue traces respectively. Horizontal smooth pursuit was similar, but saccadic activity tended to vary somewhat more across subjects. The panel on the right shows pursuit activity obtained approximately 2 hours after landing. Saccadic activity, composed primarily of what we have termed “catch-up” saccades, was increased. That is, rather than anticipating the position (or velocity) of the target, the subject lagged behind the pursuit stimulus.

Figure 5.3-9 shows smooth pursuit tracking in the horizontal plane. The panel on the left indicates tracking 10 days before flight (L-10). Tracking on landing day (R+0) is on the right panel. From the top to the bottom are presented the target wave form, the horizontal eyes, eye velocity, eye error velocity, and eye error position. Eye error velocity was derived by taking the difference between eye velocity and target velocity, and eye position from target position. The increase in saccadic activity is clearly visible between preflight and postflight values. For the most part, the saccadic activity present in the postflight trace represents anticipatory saccades, when the subject was capable of anticipating target position and velocity. Of particular interest is the large error observed in the velocity and position error traces. This error results primarily from saccadic activity. When error was applied in the position domain, it was possible to infer the amount of time the subject spent on the target.

The position error from Figure 5.3-9 is plotted in Figure 5.3-10. It shows integrated cumulative error (total area/time) as a function of the amount of time the smooth pursuit target was not within $\pm 1^\circ$ of foveal center. The postflight (R+0) retinal error was more than twice that observed before flight (L-10). Figure 5.3-11, adapted from Leigh and Zee [75], shows the degradation in acuity with target distance from foveal center. From this figure it is clear that acuity decreases by more than 50% when the target falls beyond the $\pm 1^\circ$ band.

Smooth Pursuit, Eyes Only – Summary Gaze Error and Saccadic Activity

Figures 5.3-12, 5.3-13, 5.3-14, and 5.3-15 show the relationship between saccadic activity and gaze error for four representative subjects. These subjects were selected because they represented examples of a relatively large change through modest or no change. Figure 5.3-12 shows the total number of saccades, both anticipatory and catch-up, observed over three complete cycles at 0.33 Hz of smooth pursuit for both the horizontal and vertical planes. Also shown are the averages of the four subjects with associated standard error of the mean (SEM). While not all subjects showed an increase in total saccades between preflight baseline and postflight measurements, and some actually showed a decrease, there was an overall trend toward increased saccadic activity after flight. It is

interesting to note that there were considerably more saccades in the vertical plane than in the horizontal plane, and that three of the four subjects showed an increase in vertical saccades.

The total saccade count, illustrated in Figure 5.3-12, is composed of both anticipatory saccades, where eye movements jump ahead of the predictable target, and catch-up saccades, with eye movements that lag and must move rapidly to lock on to target once the target has advanced ahead of the pursuit eye movement. Figure 5.3-13 shows the total number of catch-up saccades for horizontal and vertical pursuit tracking during preflight and postflight measurement sessions. Note that overall, the number of catch-up saccades increased by as many as 15 between horizontal plane testing before and after flight. Interestingly, there were more preflight catch-up saccades in the vertical plane than in the horizontal plane before and after flight. However, there was a slight decrease in catch-up activity between preflight and postflight saccades in the vertical plane, across all four subjects.

The relationship between catch-up and anticipatory saccades can be seen in Figures 5.3-13 and 5.3-14. While the total number of catch-up and anticipatory saccades was independent, there was a tendency to decrease anticipatory saccades when catch-up saccadic activity was high. The inverse was also observed. Note that this relationship is evident between catch-up and anticipatory saccades in the vertical plane.

Both the total number of saccades and their amplitude combine over time to create cumulative gaze error. Figure 5.3-15 shows the dramatic increase in cumulative retinal error between preflight and postflight testing in both the horizontal and vertical plane. For cumulative gaze error time calculations, deviations of $\pm 2^\circ$ from estimated foveal center were used, rather than the $\pm 1^\circ$ band width illustrated in Figure 5.3-9. Note that there were substantial increases in total error between preflight and postflight measurements, and that the increases, as expected, were greater in the vertical than in the horizontal plane. The immediate operational impact of increased gaze error was reduced visual acuity. Referring to Figure 5.3-11, and using the $\pm 2^\circ$ error band, these four subjects, on average, were off target over 50% of the time, and visual acuity was reduced by more than 75% from that expected based on preflight measures.

Smooth Pursuit – Gain and Phase

The position results, depicted in Figures 5.3-8 and 5.3-9, indicate the efficacy of the saccadic and smooth pursuit systems acting together to maintain gaze on target. The preflight gains were all near 1.0, and the only apparent phase differences were from small head movements which had insignificant gain. The postflight position gains were slightly reduced (Figure 5.3-9), suggesting that the saccadic system did contribute somewhat to the reduction of gaze position errors, but it could not contribute enough

to maintain gaze on target after flight, and may have contributed to pulling gaze away from the target (Figure 5.3-15). These observations are summarized for four subjects in Figure 5.3-16.

When the saccades were removed by processing the data in the velocity domain, the efficacy of the smooth pursuit system acting alone was observed. Before flight, the performance of the smooth pursuit system was comparable to that observed when saccades were available, indicating that there was a very small saccadic contribution to the horizontal maintenance of gaze during eyes only (smooth pursuit) tracking. After flight, there was a much larger (as much as 50%) decrement in the gain of the gaze wave form, indicating that the saccadic system was necessary to augment the postflight smooth pursuit response and reduce gaze position errors.

From the vertical smooth pursuit results depicted in Figure 5.3-17, it is apparent that gaze position was well maintained on target by contributions from both the saccadic and smooth pursuit systems. However, when saccades were removed, the performance of the smooth pursuit system alone was revealed (Figure 5.3-17b). Significant decreases in gain indicate that for vertical smooth pursuit, the smooth pursuit system relied on contributions from the saccadic system to keep the eyes directed toward the target, even before flight. This decrement in vertical plane performance, relative to horizontal tracking, is generally observed among the normal population. After flight, there was a larger attenuation of gain (as much as 80%), suggesting that there was an even stronger reliance on the availability of the saccadic system to generate eye movements to match the line-of-sight with the target. Even with the saccadic system available, postflight position gains depicted wide variability. This suggests that crew members, especially subject B, adopted different head stationary tracking strategies postflight that relied on the saccadic system in varying ways.

Eye and Head Sinusoidal Tracking

Figure 5.3-18a illustrates the effect of spaceflight on pursuing a predictable target of changing velocity, with both head and eyes. During sinusoidal eye-head tracking, the subject tracks a sinusoidally moving target with both the head and eyes, and the vestibulo-ocular reflex responds to head motion and is responsible for maintaining fixed gaze despite head motion. Therefore, the ability to track moving targets with combinations of eye and head movements requires that the reflexive command signals from the VOR in some way be canceled or suppressed to allow gaze to change along with the target. For cases of eye-head tracking, the VOR is actually an unwanted neurological command signal that must be overcome. However, phasic differences between the head and the target often make use of the VOR. In Figure 5.3-18a the left panel shows preflight tracking of the laser point stimulus at 0.33 Hz, 20° peak. Target, head, eye, and gaze are

represented by the black, red, blue, and green traces, respectively. The VOR is present before flight, and gaze only slightly lags the target. It is also apparent that the VOR is functional, and that gain is close to unity, evident not only in the gaze peak amplitude, but also in the lack of saccadic activity in the gaze trace. After flight (R+0) the saccadic activity was apparent, driven by both the catch-up and anticipatory saccades observed during smooth pursuit results (Figure 5.3-18a right panel). Spaceflight clearly increased both gaze error and gain, whereas phase lagged.

Figure 5.3-18b shows a single cycle from a subject different than that illustrated in Figure 5.3-18a. The primary difference between these two examples is the suppression of the VOR during the preflight (L-10) testing (Figure 5.3-18b). Postflight, gaze may in fact be maintained because the VOR compensated for the reduced peak-to-peak displacement (reduced velocity and gain) of the head.

Smooth Pursuit, Eyes and Head – Saccades and Gaze Error

Figure 5.3-19 shows the total number of saccades, before and after flight, over three complete cycles of the sinusoidally moving laser point stimulus, with a 20° peak displacement in the vertical and a 30° peak displacement in the horizontal planes. The same four subjects analyzed above in eyes-only smooth pursuit were used. Vertical bars, superimposed on the average of the four subjects, represent SEM. In keeping with the eyes-only smooth pursuit results, there was an overall average increase in saccadic activity after flight. Also in the horizontal plane there was an average of 35 saccades after flight as compared to 19 before flight. Figure 5.3-20 shows the number of catch-up saccades, and Figure 5.3-21 the number of anticipatory saccades, over three complete cycles. In both cases there was an overall increase in both types of saccadic activity, in both planes and across spaceflight conditions postflight, compared to the preflight value. However, unlike the saccadic activity in the eyes-only pursuit, most of the activity with the head and eyes acting together was clearly related to catch-up saccades. Not surprisingly, most of the overall saccadic activity, both before and after flight, was in the vertical plane. With eye and head sinusoidal tracking at 0.33 Hz, the postflight cumulative gaze error in the horizontal plane increased for two subjects and decreased for two. The overall effect was a slight decrease across all four subjects, with large variability. Gaze error was considerably larger in the vertical than in the horizontal plane (Figure 5.3-22).

Eye and Head Pursuit Tracking – Gain and Phase

Figure 5.3-23 depicts the gaze gains and phase differences with respect to the target, as well as the corresponding eye and head movement gain and phase components of gaze. For horizontal eye-head tracking before flight, the

minimal differences between the gaze position and velocity data indicate that saccadic contributions to eye-head tracking were small. On-target gaze data were obtained from a strategy that combined head movements (which led the target) with lower amplitude eye movements (which lagged behind the target). This head-lead/eye-lag strategy was a general trend with considerable variability among subjects. The postflight position data were quite similar to the preflight position data, although there was a slight tendency after flight toward larger contributions to gaze from head, and consequently less contributions from eye.

Two interesting observations can be made from the postflight velocity data. First, the slight decrease in gain for gaze velocity after flight, compared to before flight, can be attributed to an increase in the contributions from the saccadic system. Second, the significant eye velocity phases (~90-180°) indicate that the combined eye movement contributions from the VOR and the smooth pursuit system caused the eye to move opposite of the target and the head. This is important because eye velocity counter to that of head velocity is indicative of a residual VOR command signal that is not being sufficiently canceled by the smooth pursuit system. Thus, for eye-head tracking after flight, there was a residual VOR that was not being completely canceled by the smooth pursuit system. This presumably occurred either because of decrements in the ability of the smooth pursuit system to generate “normal” VOR cancellation signals, or because VOR gain had increased to a point where normal VOR cancellation signals were no longer effective in providing complete cancellation.

Preflight, vertical eye-head tracking gains (Figure 5.3-24) indicated that subjects were able to match sinusoidal target motion fairly well using the full complement of smooth pursuit, VOR, and saccadic eye movements. Again, the major contribution to gaze came from head movements, while eye movements played a lesser role in supplementing the head and correcting for head tracking errors. By comparing preflight position and velocity data it is apparent from the decrease in gaze gain that the saccadic system is necessary to correct for position errors. The position errors apparently result from incomplete tracking with the combination of head movements, smooth pursuit eye movements, and the VOR during vertical tracking tasks.

Postflight, position gains were reduced slightly in three subjects, with most of the gaze tracking contribution coming from head movement. Subject B had a large head phase lead and thus needed a higher gain eye lag to compensate. The dramatic reduction in overall gaze gain, with the saccades removed in the velocity domain, shows that saccades played an important role in maintaining gaze position on target. Also, the large phase shifts (~180°) of the eye velocity signals show that the smooth (non-saccadic) eye movements were driven in a direction opposite of the head (and target), suggesting incomplete VOR

cancellation or suppression. Incomplete attenuation of the VOR signal during horizontal tracking suggests that either (1) the smooth pursuit signal was no longer capable of canceling the normal VOR command signal, (2) the VOR gain had increased to a level where even a normally adequate smooth pursuit cancellation signal was no longer effective, or (3) a combination of the two occurred.

All of these data indicate that saccades were important to maintain gaze directed toward the target during postflight tracking of a sinusoidally moving target, both with the head stationary and with the head assisting in tracking. Because sequences of saccades are generated in more or less a "stair-step" pattern, using them in any significant way to track smoothly moving targets results in periods of clear vision intermixed with intervals in which the eyes are stationary while the target moves (e.g., Figure 5.3-24, R+0). The latter circumstance results in slip of the target image on the retina and thus, reduced visual acuity. The significant postflight reliance on the saccadic system suggests that crew members were not seeing with a clear, smooth vision, but rather in time-displaced "snapshots," sampled at the conclusion of each saccade.

Finally, the large phase shifts associated with the eye velocity data during eye-head tracking after flight, show that the VOR was not being adequately canceled or suppressed. Either there was a reduction in overall efficacy of the smooth pursuit system during this task, or a substantial increase in VOR gain. If the latter were true, one might expect that some crew members would adopt a tracking strategy that moved the head in the opposite direction of the target, thereby using the increased gain VOR as a tracking mechanism to actively drive the eyes toward the target. At this point, none of the data suggest such a counter-directional head movement strategy.

Pursuit Tracking of an Unpredictable Velocity Ramp

The sinusoidal pursuit tasks discussed above are predictive in nature, each being a recurring cycle that once began, continues in the same fashion until the trail ends. The pursuit tracking of velocity ramps was an unpredictable task, with the velocity, peak displacement, and plane of the ramps counterbalanced, using a systematic randomization scheme. The end result was that they were clearly unpredictable in terms of direction of movement, velocity, and peak amplitude. Unlike the predictable sinusoidal trials, where velocity was constantly changing although peak velocity remained constant, the velocity steps maintained a constant velocity until peak amplitude was reached. The constant velocity factor may have been a significant component in the results obtained with this stimulus. Information illustrated in Figures 5.3-25-5.3-30 is from a single subject, representative of all subjects tested with this protocol.

Figures 5.3-25 and 5.3-26 illustrate pursuit tracking with the eyes only, using a low velocity (15°/sec), large displacement (30°) position ramp stimulus to the subject's

right in the horizontal plane. Before flight (Figure 5.3-25), the subject easily tracked the ramp stimulus (black trace) with the eyes (blue trace) while the head was held stationary (green trace). There was a characteristic delay in the eye movement following initiation of the target stimulus, after which the eye quickly locked onto the target. After the target reached its maximum amplitude, the eye continued to move briefly in the direction of previous target displacement and was returned to the final target position with a small accurate saccade. After flight (Figure 5.3-26), the response pattern was qualitatively the same as that observed before flight, showing no difference in response due to microgravity exposure. This same response pattern was noted when a much higher velocity stimulus was used (30°/sec) with a final target displacement of 30° (Figures 5.3-27 and 5.3-28).

Figures 5.3-29 and 5.3-30 illustrate pursuit tracking, with both the eyes and head, using unpredictable large displacements and velocities (30° and 30°/sec respectively) to the subject's left in the horizontal plane. The primary difference between the eyes only and head plus eyes tracking was a constant deviation of the eye position (red trace) that did not return to 0°. The difference between preflight and postflight response when both the head and eye tracked the ramp target was a decrease in head velocity, requiring a compensatory eye saccade to maintain gaze on the target during the postflight testing.

Target Acquisition

Typically, an orienting gaze movement, initiated to bring a selected part of the visual world onto the fovea, consists of an eye movement saccade and a head movement followed by a reflexive compensatory eye movement driven by the VOR. In the usual sequence, a saccade directs the eye either onto the target for targets with a small angular displacement or toward the target when the angular displacement exceeds either the physical or physiological limits of eye rotation. The head, being a larger mechanical object with greater inertia compared with the eye, typically moves after the eye has moved in the orbit. The head movements excite the semicircular canals and produce an eye movement through the VOR that is opposite in direction and velocity to that of the head. The compensatory VOR returns the eye to the primary straight ahead position in the skull's orbit, exchanging the head's final angular position for the initial eye saccade. Most observations before flight used a normal sequence of head and eye movements to assist in target acquisition. Immediately after flight, strategies were used to bring gaze onto a target that did not necessarily correspond to those observed by other investigators who have studied changes in strategies associated with verbal instructions and target predictability.

After flight, there was a consistent trend (Figure 5.3-31) for the head movement to the target to be delayed for

those targets near or beyond the effective oculo-motor range ($\pm 50^\circ$), as defined by Guitton and Volle [76]. Such a delay could result in a VOR following the initial eye saccade that would tend to pull gaze off target. Figure 5.3-31a shows head, eye, and gaze position in the left-most panel, and velocity traces for each of these parameters in the rightward panel for preflight acquisition of a vertical target in the upward direction that is beyond the EOM. Figure 5.3-31b shows the same parameters for a postflight (R+0) target acquisition. When the preflight parameters are compared with those obtained, several clear differences are apparent. First, postflight the head movement to the target is delayed relative to preflight, and the final position of the head, as well as the head's velocity, are reduced. As a consequence, the VOR was initiated at an inappropriate time, pulling gaze off target during the postflight measurement. This postflight delay (and low velocity head movement) induced a series of large anti-compensatory saccades that were required to direct gaze back onto the target.

Figure 5.3-32 illustrates the acquisition of a target beyond the EOM, in the vertical plane throughout all flight phases. As can be seen in the preflight trial, the subject used the eyes to attempt acquisition of the target. The eyes were moved prior to the head, and gaze was established with the eyes' position. Once the head began to move, the visually assisted vestibulo-ocular reflex (VVOR) was established and the reflex pulled gaze off the target. Both the head and a corrective eye saccade were then used to maintain gaze. During the flight, a different strategy was developed. The eye was still used to establish gaze, but the head movement was greatly reduced in both velocity and displacement (flight days 1 and 8). The number of saccades made by the eyes and the velocity of these saccades did not represent a typical VVOR response, but had a higher than normal gain. The responses for R+0 and R+1 days show most of the strategy components, such as attainment of target with eyes, low head velocity, and multiple saccades, developed during the flight. A return to preflight levels was observed by R+4.

A preliminary attempt was made to combine data across trials and subjects. The results obtained on a randomly-selected five subjects follows; however, because the strategies selected by each astronaut were different, traditional descriptive and multivariate statistical analysis washed out individual trends. Traditional analysis was therefore abandoned in favor of attempting to establish strategy groups. One approach was to place responses in groups identified by head and eye movement patterns identified by Zangemeister and Stark [77].

For horizontal gaze shifts, the delay between the start of eye and head movements was significantly different only for the 68° target (preflight 0.010 ± 0.076 sec vs. postflight 0.070 ± 0.102 sec, $p=0.015$; indicates head leads eye). For vertical target acquisition, this delay was again only significant for targets approaching the limits of the EOM

range ($\pm 50^\circ$), and only for targets in the upwards direction (preflight 0.042 ± 0.077 sec vs. postflight 0.177 ± 0.184 sec; $p=0.045$). For all other targets in the vertical plane, including those in the downward direction, there was a strong but insignificant trend for the head to be delayed during postflight testing. There was a significant difference in two of the five subjects for both horizontal and vertical targets within the EOM range, resulting in an average head delay of approximately 50 msec, when data from all five subjects were pooled.

The maximal eye and head velocities determine the time to bring gaze on target when the eye and head movement strategies function correctly and the interaction between the saccadic and VOR eye motion is sequenced correctly. After flight, the eye and head maximal velocities were found to be consistently below those observed before flight. For small target displacements ($\leq 20^\circ$) the difference was not significant, but showed the same trend observed for eye and head velocities made to targets beyond the EOM range. For the 30° targets both eye and head velocities were only 80% of the preflight value (preflight: head = $127 \pm 35^\circ/\text{sec}$ vs. postflight $105 \pm 32^\circ/\text{sec}$, $p=0.037$; eye = $329 \pm 46^\circ/\text{sec}$ vs. postflight $274 \pm 71^\circ/\text{sec}$, $p=0.007$). For the 68° target in the horizontal plane, a reduction of more than 30% was observed for both head and eye velocity (preflight: head = $196 \pm 36^\circ/\text{sec}$ vs. postflight $150 \pm 44^\circ/\text{sec}$, $p=0.003$; eye = $305 \pm 35^\circ/\text{sec}$ vs. postflight $208 \pm 60^\circ/\text{sec}$, $p=0.0005$).

The overall means of the final horizontal eye and head amplitudes before flight were not significantly different than after flight. However, postflight the eyes tended to contribute more to gaze displacement than preflight. Three of the five subjects showed smaller head amplitudes ($>20\%$) during postflight testing for targets beyond the EOM range. Vertical velocities for upward target acquisition trials also decreased, although significance levels were smaller. No differences were found for the 15° target. For the 20° target head velocity remained the same, but eye, and hence gaze, velocity decreased (gaze = preflight $343 \pm 76^\circ/\text{sec}$ vs. postflight $274 \pm 90^\circ/\text{sec}$, $p=0.021$; eye = preflight $330 \pm 82^\circ/\text{sec}$ vs. postflight $244 \pm 88^\circ/\text{sec}$, $p=0.038$). Both eye and head velocities decreased with targets beyond the EOM range, but were more variable than those within the EOM range. These differences occurred only for upward movements. For the near target (15°), mean eye and corresponding gaze velocity increased after flight (eye: preflight $308 \pm 82^\circ/\text{sec}$ vs. postflight $351 \pm 238^\circ/\text{sec}$), while head velocity remained the same.

One method of illustrating and qualitatively describing the changes in strategy, rather than pooling subject data, involves determining the type of gaze movement evoked. Zangemeister and Stark [77] have attempted to do this by determining the timing sequence between the command to move the head and the command to move the eyes. They have determined that gaze shift movements fall into four distinct types with respect to eye-head

latencies. In an attempt to group gaze shift strategies in the target acquisition task, we adopted a method developed by Wolfgang Zangemeister and Lawrence Stark. This method identifies five distinct groupings, called Stark Types, that are differentiated by the latency of eye movement onset, specifically the difference between the time of eye muscle stimulation (tEs) and the time of neck muscle stimulation (tHs), relative to head movement onset.

Because head or eye EMG were not measured, the time of eye and neck muscle stimulation were derived from measured values of eye movement onset (tEo) and head movement onset (tHo). To do this, the relative mass of the eye and head were taken into account. Since the mass of the eye is small, we assumed that the time of eye muscle stimulation and time of measured eye movement onset is simultaneous, and that the latency between the two is negligible ($tEo - tEs = 0$). However, the head has a much larger mass and does not move instantaneously after neck EMG excitation. Zangemeister and Stark found that the time of neck muscle stimulation (tHs) and time of head movement onset (tHo), are delayed by 50 msec. Therefore, 50 msec must be subtracted from the measured time of head movement onset ($tHo - 50 \text{ msec} = tHs$) to get time of neck muscle stimulation (Figure 5.3-33).

The latency information, obtained from the formula ($tEs - tHs$), can be used to group each gaze shift into either Stark Type I, II, IIIa, IIIb, or IV, depending upon where the latency falls in the time ranges defined by Zangemeister and Stark (Table 5.3-3). Table 5.3-3 shows times of EMG latencies that define each Stark Type. However, because these are physiological systems and neck and eye EMG are not being measured, it is highly unlikely that the latency will be exactly equal to zero. Therefore we have chosen a time window, Δt , of ± 25 msec around tHs where differences in tEs and tHs are effectively equal. So to be a Stark Type I, the difference between neck and eye muscle stimulation must fall within the ± 25 msec Δt time window (Figure 5.3-34). Stark Type II is defined as a late head movement, where the difference between neck and eye muscle stimulation falls before the ± 25 msec Δt time window (Figure 5.3-35). This type was seen very rarely in our study because the subject was instructed to move eyes and head as quickly, but accurately, as possible to acquire the target. Stark Type IIIa is defined as an early head movement where the latency of neck and eye stimulation must be in the range following

Table 5.3-3. Classification of Stark types

Type	Electromyogram (tEs - tHs)
I	0
II	Negative
IIIa	0 - 150 msec
IIIb	150 - 500 msec
IV	>500 msec

the $+\Delta t$ time window to 150 msec (Figure 5.3-36). This means that the head is commanded to move up to 150 msec before the eye is commanded. This is the most common type that occurred in our study, with occasional appearance of Type IIIb. Stark Type IIIb is also defined as an early head movement relative to the eye, but the head is commanded to move 150 msec to 500 msec before the eye is commanded (Figure 5.3-37). This type usually produces an initial eye movement in the opposite direction of the head before a saccade brings the eye toward the target. Stark Type IV is defined as a gaze shift where head movement completely governs the eye movement (Figure 5.3-38). It can be either a suppression of the VOR where the eye is carried to the target by the head, or without suppression of the VOR where the head first reaches the target and gaze is shifted to target with a late eye saccade. This gaze shift type, never seen in our study, would mean that the crew member was not doing the task correctly. When the Stark gaze shift types are represented in either the phase plane or parametric plots, it is possible to generate gaze plane representations that clearly allow the establishment of gaze shift errors. One of the most useful gaze shift errors to examine is that generated as a function of time. Figures 5.3-39 through 5.3-45 illustrate the process of establishing gaze-shift error.

Figures 5.3-39 and 5.3-40 show two different gaze shift strategies that were used to obtain a target beyond the EOM. Figure 5.3-39 was generated from data obtained before flight and shows a head movement that begins synchronous with, or perhaps just slightly before, movement of the eye towards the target. This type of movement corresponds to a Stark Type I strategy. The target acquisition illustrated in Figure 5.3-40 was obtained after flight and shows an eye movement towards the target just prior to movement of the head (Stark Type III). The primary difference between the preflight and postflight strategies is clearly seen in the velocity of the head, the final position of the head, and the number of saccades generated prior to gaze stability. Before flight, the eye made a major saccade toward the target, assisted by the movement of the head. A normal VVOR was established with a gain just slightly greater than one. After flight, there were multiple saccades prior to final gaze position, and the gain of these saccades was much greater than unity, indicating that they were not a component of the VVOR.

The difference between these two responses is clearly illustrated when gaze is plotted as a phase plane (Figures 5.3-41 and 5.3-42). Total gaze error can be derived from integrating the area represented in blue (head position 0° to maximum gaze displacement). However, gaze error is a function of time and can be best illustrated by Figures 5.3-43 and 5.3-44. Three major factors contribute to gaze error. These are: (1) response latency, (2) time taken to achieve final gaze position, and (3) the number of saccadic eye movements generated. The area bounded by red in both figures represents the area to be integrated. The preflight gaze error (Figure 5.3-43) was approximately

$20^\circ \times \text{sec}$ and the postflight gaze error (Figure 5.3-44) was $54^\circ \times \text{sec}$. Another way of illustrating gaze error as a function of time is presented in Figure 5.3-45.

Figure 5.3-46 represents the gaze error for a representative subject who displayed large gaze error as a function of flight days. The shaded area is the average total gaze error before flight, the day of landing (R+0), and six days later (R+6). Total gaze error over time increased dramatically on R+0, and on R+6 was still above that observed before flight. Absolute values of gaze error at R+6 were as much as 40% above the preflight values, particularly for the targets beyond the EOM. Figure 5.3-46 also clearly demonstrates that total gaze error was greatest for those targets that were beyond the EOM, and that as postflight recovery occurred, the differences between the targets beyond the EOM and those within the EOM became less.

Perhaps one of the most important aspects of determining total gaze error as a function of time is its use as an index of performance. When it is critically important to obtain a target in the shortest amount of time, large gaze errors result in less accurate target acquisition responses over time. It may also be used to predict postflight or in-flight performance using preflight behavior. This hypothesis was tested by determining the absolute gaze error as a function of time from preflight trials, using only those targets beyond the EOM, then relating the absolute gaze error to the head and eye velocity in the vertical plane for a specific trial obtained during target acquisition. In relating gaze error to head and eye velocity, the error was categorized in terms of either a large or small gaze error, with a small gaze error being the smallest value relative to a typical Stark Type III response.

Figure 5.3-47 shows preflight gaze error as a function of the head and eye velocity associated with the target acquisition response where the gaze error was associated. Based on this information it is not possible to use preflight gaze error to predict postflight performance. When the gaze error derived from the in-flight responses was evaluated as a function of vertical head and eye velocities measured postflight (Figure 5.3-48), a slight trend was apparent. Although large gaze errors appeared to be associated with lower vertical eye velocities, the absolute gaze errors did not clearly separate into distinct groups.

When absolute gaze errors as a function of time were associated with postflight vertical head and eye velocities, a clear trend was apparent (Figure 5.3-49). Large gaze errors were more likely to be associated with lower head and eye velocities, while small gaze errors were related to higher head and eye velocities. Among other things, this finding suggests that the neural strategies adopted during adaptation to microgravity may not have been optimal for postflight performance. Astronauts adopting a strategy of higher head and eye velocities may have had less difficulty and reduced gaze error.

Gaze Stabilization

Several parameters of gaze stabilization were computed, such as VVOR gain which was expressed by the slope of eye versus head velocity after saccade removal, gaze error after the head movement, and maximal velocities and amplitudes of eye and head. Only the decrease in vertical head peak velocity for downward movements showed a significant difference (preflight $80.9 \pm 15.4^\circ/\text{sec}$ vs. postflight $64.0 \pm 18.7^\circ/\text{sec}$). In general, postflight performance required a large saccadic eye movement to bring the eye back on target once vision was restored for the first trial or two. The saccadic correction is illustrated by comparing the preflight response (Figure 5.3-50a) with the postflight response (Figure 5.3-50b). Subsequent postflight trials showed an immediate trend, in all planes and directions, toward preflight baseline values, usually returning to normal within four gaze stabilization trials. Postflight performance was also often disturbed by saccadic eye movements (Figure 5.3-51). Subjects often locked their eyes in the head when starting a head movement. This required following saccades to bring the eye back on target, even when vision was not present.

The early in-flight gaze stabilization trials were similar to those observed before flight. However, measurements taken late in flight were more analogous to those obtained immediately after flight. Gaze stabilization was also the only VHM performed during entry, landing, and immediately after landing, while crew members were still in the space craft and in their space suits. During orbit to maximal sustained gravity (Figure 5.3-50c), the phase of entry where the change in gravitational forces was the greatest, there was not a corresponding VOR for the head movement in both the horizontal and vertical planes. It was at this stage of flight that small head movements frequently evoked sensations of either self-motion or surround motion that were linear in response to an angular input. One probable explanation for the lack of VOR and subsequent gaze drift is that the eye movement was compensating for the perception of self-motion and surround motion.

Sinusoidal Head Shakes

During sinusoidal head shakes, the subject maintained visual fixation on the target, or when vision was occluded, the subject attempted to maintain fixation on the target while smoothly oscillating the head in either the horizontal or vertical plane, in cadence with an audio tone that was sinusoidally modulated at each of four frequencies (0.2, 0.3, 0.8, and 2.0 Hz). Angular displacement of head oscillation was selected by the subject for comfort. When performing the analysis of the head shakes, special attention was paid to cross axes head movements, corresponding compensatory eye movements, and changes in head movement control. Figure 5.3-52 demonstrates the yaw cross

axes head movements when the head was pitched at each of the four different frequencies. While small, there was considerable secondary cross axis yaw movement. As expected, the greatest cross axis yaw movements occurred at the lowest frequency, and decreased as frequency was increased to 2.0 Hz (Figure 5.3-53). The larger overall cross-axis movement, when the subject had visual feedback regarding head position, was not expected. With the exception of 0.20 Hz, the postflight performance between vision and no vision was reversed relative to preflight values, indicating that after flight the removal of visual feedback resulted in the maintenance of head plane to the primary axis. There was no significant evidence of roll head movements when the head was pitched.

Figures 5.3-54 through 5.3- 61 illustrate the pitch head shakes in phase plane plots. Presented in this fashion, it is easy to see peak to peak displacement, velocity, head precession, and cycle-to-cycle consistency. Figures 5.3-54 through 5.3-57 show head shakes with vision before (L-10) and after space flight (R+0) at each of the four frequencies, when the subject had a visual reference. Displacement was greatest for the lower frequencies and decreased as the frequency increased. The inverse was true for velocity. There was very little evidence of precession, as the head did not progressively move from its original peak displacements, centered around up and down during the head shakes, to seek a new center. With the exception of the 0.20 Hz head shake, there was little change in either amplitude or velocity as a function of the flight phase.

Figures 5.3-58 through 5.3-61 show the results when vision was removed (occluded with the eyes open). Like the head shakes with vision, those without vision showed a progressive decrease in displacement with an increase in head shake frequency, and an increase in velocity as frequency increased. Unlike the head shakes with vision, there was a consistent trend to decrease head shake velocity, more strongly evidenced at the lower frequencies, immediately after space flight (R+0). There was also evidence, again at the lower frequencies, for precession to occur. Precession is important because it points to a loss or change in crew member spatial orientation. The strongest trend for precession occurred at the higher frequencies.

Head Movement Control

As evidenced by investigations of changes in the major postural muscles [16], spaceflight is believed to have a major impact on the sensory-motor systems responsible for balance and locomotion. Driven by the stimulus rearrangement of the flight environment, the newly adapted postural control is more suitable for microgravity than the Earth's gravitational forces. Loss of muscle mass and subsequent decreases in strength may also play a role in the changes observed in sensory-motor control as a function of spaceflight. All of these factors that may affect the major postural

muscles may also affect control of the neck muscles. Specifically, there is a possibility that sensory/motor nerve terminals may undergo changes that would make control of the neck more difficult in the Earth's environment following spaceflight. One possible way to investigate these changes is to examine head movement control after flight and compare it to preflight functional performance.

Figure 5.3-62 shows horizontal head position as a function of time during calibration procedures of the rate sensors used to measure the head position in space. The green trace shows a preflight trial (L-10). The red trace represents data obtained during the first head movement calibration trial immediately after flight (R+0), and shows that head position overshoot the calibration target. This overshoot reflects the lack of head control, and suggests that motor performance was compromised as a result of: (1) changes in descending vestibular information, and/or (2) a change in the substrate of the sensory-motor physiology. Figure 5.3-63 shows data for a second subject that did not display the changes evident in Figure 5.3-62. The differences could be due to head velocity, assuming that changes in the sensory-motor substrate were equal for both subjects. Also, the velocity of head movements could be different; the higher the velocity, the less control is available. Figure 5.3-64 depicts the velocity for head position shown in Figure 5.3-62. Figure 5.3-65 shows the velocity for head position plotted in Figure 5.3-63. The postflight velocity shown in Figure 5.3-65 was approximately 40% less than that depicted in Figure 5.3-64 for a different subject.

REFERENCES

1. Shaw RE, Kugler PN, Kinsella-Shaw J. Reciprocities of intentional systems. In: Warren R, Wertheim AH, editors. Perception and control of self-motion. Hillsdale, New Jersey: Lawrence Erlbaum; 1990. p 579-620.
2. Mittelstaedt H, Fricke E. The relative effect of sacular and somatosensory information on spatial perception and control. *Adv Oto-Rhino-Laryngol* 1988; 42:24.
3. von Gierke HE, Parker DE. Differences in otolith and abdominal viscera graviceptor dynamics: Implications for motion sickness and perceived body position. *Aviat Space Environ Med* (in press).
4. Howard IP. Human visual orientation. New York: John Wiley & Sons; 1982.
5. Cornilleau-Peres V, Droulez J. Three-dimensional motion perception: sensorimotor interactions and computational models. In: Warren R, Wertheim AH, editors. Perception and control of self-motion. Hillsdale, New Jersey: Lawrence Erlbaum; 1990. p 81-100.

6. Bock O. Coordination of arm and eye movements in tracking of sinusoidally moving targets. *Behav Brain Res* 1987; 24:3-100.
7. Calvin WH. *The cerebral symphony*. New York: Bantam Books; 1989.
8. Parker DE, Parker KL. Adaptation to the simulated stimulus rearrangement of weightlessness. In: Crampton GH, editor. *Motion and space sickness*. Boca Raton, FL: CRC Press; 1990. p 247-62.
9. Howard IP, Templeton WB. *Human spatial orientation*. London: John Wiley & Sons; 1966.
10. Guedry, F. Psychophysics of vestibular sensation. In: Held R, Liebowitz HW, Tuerber HL, editors. *Handbook of sensory physiology; vestibular system part 2: psychophysics and applied aspects and general interpretations*. Berlin: Springer Verlag; 1974. p 3-154.
11. Howard IP. The perception of posture, self motion, and the visual vertical. In: Boff KR, Kaufman L, Thomas JP, editors. *Handbook of perception and human performance, vol 1*. New York: John Wiley & Sons; 1986. p 18-1 to 18-62.
12. Mittelstaedt H. A new solution to the problem of subjective vertical. *Naturwissenschaften* 1983; 70:272-81.
13. Parker DE, Poston RL. Tilt from a head-inverted position produces displacement of visual subjective vertical in the opposite direction. *Perception & Psychophysics* 1984; 36:461-5.
14. Parker DE, Poston RL, Gullledge WL. Spatial orientation: visual-vestibular-somatic interaction. *Perception & Psychophysics* 1983; 33:139-46.
15. Young LR, Oman CM, Merfeld D, Watt D, Roy S, DeLuca, C, Balkwell D, Christie J, Groleau N, Jackson DK, Law G, Modestino S, Mayer W. Spatial orientation and posture during and following weightlessness: Human experiments on Spacelab Life Sciences 1. *J Vestib Res* 1993; 3:231-9.
16. Reschke MF, Harm DL, Parker DE, Sandoz G, Homick JL, Vanderploeg JM. Physiologic adaptation to space flight: neurophysiologic aspects: space motion sickness. In: Nicogossian AE, Leach CL, Pool SL, editors. *Space physiology and medicine*. Philadelphia: Lea & Febiger; 1994. p 228-60.
17. Reschke MF, Bloomberg JJ, Paloski WH, Harm DL, Parker DE. Physiologic adaptation to space flight: neurophysiologic aspects: sensory and sensory-motor function. In: Nicogossian AE, Leach CL, Pool SL, editors. *Space physiology and medicine*. Philadelphia: Lea & Febiger; 1994. p 261-85.
18. Clément G, Reschke MF. Neurosensory and sensory-motor function. In: Moore D, Bie P, Oser H, editors. *Biological and medical research in space*. Berlin: Springer-Verlag; 1996. p 178-258.
19. Paloski WH, Black FO, Reschke MF. Vestibular ataxia following shuttle flights: effects of transient microgravity on otolith-mediated sensorimotor control of posture. *Am J Otolaryngol* 1993; 1:9-17.
20. Friederici AD, Levelt WJM. Resolving perceptual conflicts: the cognitive mechanisms of spatial orientation. *Aviat Space Environ Med* 1987; 58(9 Suppl):A164-9.
21. Harm DL, Parker DE. Perceived self-orientation and self-motion in microgravity, after landing and during preflight adaptation training. *J Vestib Res* 1993; 3:297-305.
22. Mittelstaedt H, Glasauer S. Crucial effects of weightlessness on human orientation. *J Vest Res* 1993; 3:307-14.
23. Wolfe JM, Held R. Eye torsion and visual tilt are mediated by different binocular processes. *Vis Res* 1979; 19:917-20.
24. Perterka RJ, Benolken MS. Relation between perception of vertical axis rotation and vestibulo-ocular reflex symmetry. *J Vest Res* 1992; 2:59-70.
25. Oman CM, Bock OL, Huang JK. Visually induced self-motion sensation adapts rapidly to left-right visual reversal. *Science* 1980; 209:706-8.
26. Oman CM, Balkwill MD. Horizontal angular VOR, nystagmus dumping, and sensation duration in Space-lab SLS-1 crewmember. *J Vest Res* 1993; 3:315-30.
27. Welch RB. Adaptation of space perception. In: Boff KR, Kaufman L, Thomas JP, editors. *Handbook of Perception and Human Performance, vol 1*. New York: John Wiley & Sons; 1986. p 24-1 to 24-45.
28. Berthoz A, Grantyn A. Neuronal mechanisms underlying eye-head coordination. *Prog Brain Res* 1986; 64:325-43.
29. Thornton WE, Biggers WP, Thomas WG, Pool SL, Thagard NE. Electronystagmography and audio potentials in space flight. *Laryngoscope* 1985; 95:924-32.
30. Thornton WE, Uri JJ, Moore T, Pool S. Studies of the horizontal vestibulo-ocular reflex in space flight. *Arch Otolaryngol Head Neck Surg* 1989; 115:943-9.
31. Vieville T, Clement G, Lestienne F, Berthoz A. Adaptive modifications of the optokinetic vestibulo-ocular reflexes in microgravity. In: Keller EL, Zee DS, editors. *Adaptive processes in visual and oculomotor systems*. New York: Pargamon Press; 1986. p 111-20.
32. Watt DGD, Money KE, Bondar RL, Thirsk RB, Garneau M, Scully-Power P. Canadian medical experiments on shuttle flight 41-G. *Can Aeronaut Space J* 1985; 31:215-26.

33. Benson AJ, ViÈville T. European vestibular experiments on the Spacelab-1 mission: 6. Yaw axis vestibulo-ocular reflex. *Exp Brain Res* 1986; 64:279-83.
34. Grigoriev AL, et al. Medical results of the Mir year-long mission. *Physiologist* 1991; 34:S44-48.
35. Vesterhaug S, Mansson A, Johansen TS, Zilstorff K. Oculomotor response to voluntary head rotations during parabolic flights. *Physiologist* 1982; 25:S117-18.
36. Lackner JR, Graybiel A. Variations in gravito-inertial force level affect the gain of the vestibulo-ocular reflex: implications for the etiology of space motion sickness. *Aviat Space Environ Med* 1981; 52:154-58.
37. DiZio P, Lackner JR, Evanoff JN. The influence of gravito-inertial force level on oculomotor and perceptual responses to sudden stimulation. *Aviat Space Environ Med* 1987; 58:A224-30.
38. DiZio P, Lackner JR. The effects of gravito-inertial force level and head movements on post-rotational nystagmus and illusory after-rotation. *Exp Brain Res* 1988; 70:485-95.
39. Oman CM. Personal communication. 1991.
40. Oman CM, Kulbaski M. Spaceflight affects the 1-g postrotatory vestibulo-ocular reflex. *Adv Oto-Rhino-Laryng* 1988; 42:5-8.
41. Oman CM, Weigl H. Postflight vestibulo-ocular reflex changes in space shuttle/Spacelab D-1 crew. *Aviat Space Environ Med* 1989; 60:480.
42. Oman CM, Lichtenberg, BK, Money KE. Space motion sickness monitoring experiment: Spacelab 1. In: Crampton GH, editor. *Motion and space sickness*. Boca Raton, FL: CRC Press; 1990. p 217-46.
43. Clément G, Reschke MF, Verrett CM, Wood SJ. Effects of gravito-inertial force variations on optokinetic nystagmus and on perception of visual stimulus orientation. *Aviat Space Environ Med* 1992; 63:771-77.
44. Guedry FE. Orientation of the rotation-axis relative to gravity: Its influence on nystagmus and the sense of rotation. *Acta Otolaryng* 1965; 60:30-48.
45. Guedry FE. Psychophysiological studies of vestibular function. In: Neff WD, editor. *Contribution to Sensory Physiology*. New York: Academic Press; 1965.
46. Benson AJ, Bodin MA. Comparison of the effect of the direction of the gravitational acceleration on post-rotational responses in yaw, pitch and roll. *Aerospace Medicine* 1966; 37:889-97.
47. Bodin MA. The effect of gravity on human vestibular responses during rotation in pitch. *J Physiol* 1968; 196:74-75.
48. Kozlovskaya IB, et al. The effects of real and simulated microgravity on vestibulo-oculomotor interaction. *The physiologist* 1985; 28(6):51-56.
49. Thornton WE, Moore TP, Uri JJ, Pool SL. Studies of the vestibulo-ocular reflex on STS 4, 5 and 6. NASA Technical Memorandum 1988; 100 (461):42.
50. Uri JJ, Linder BJ, Moore TP, Pool SL, Thornton WE. Saccadic eye movements during space flight. NASA Technical Memorandum 1989; 100(475):9.
51. Laurutis VP, Robinson DA. The vestibulo-ocular reflex during human saccadic eye movement. *J Physiol (Lond)* 1986; 373:209-233.
52. Guitton D, Volle M. Gaze control in humans: eye head coordination during orienting movements to targets within and beyond the oculomotor range. *J Neurophysiol* 1987; 58:427-59.
53. Bloomberg J, Melvill Jones G, Segal B, McFarlane S, Soul J. Vestibular-contingent voluntary saccades based on cognitive estimates of remembered vestibular information. *Adv Oto-Rhino-Laryng* 1988; 41:71-75.
54. Bloomberg J, Melvill Jones G, Segal B. Adaptive modification of vestibularly perceived self-rotation. *Exp Brain Res* 1991; 84:47-56.
55. Israel I, Berthoz A. Contribution of the otoliths to the calculation of linear displacement. *J Neurophysiol* 1989; 62:247-63.
56. Barnes G.R. Visual-vestibular interaction in the coordination of eye and head movements. In: Fuchs & Becker, editors. *Progress in oculomotor research*. New York: Elsevier; 1981. p 299-308.
57. Halmagyi GM, Gresty MS. Clinical signs of visual-vestibular interaction. *J Neurol Neurosurg Psychiatry* 1979; 42: 934-39.
58. Huebner WP, Leigh RJ, Thomas CW. An adjustment to eye movement measurements which compensates for the eccentric position of the eye relative to the center of the head. *J Vestib Res* 1992; 2:167-73.
59. Robinson DA. A model of cancellation of the vestibulo-ocular reflex. In: Lennerstrand G, Zee DS, Keller EL, editors. *Functional Basis of Ocular Motility Disorders*. New York: Pergamon Press; 1982. p 5-13.
60. Cullen KE, Chen-Huang C, McCrea RA. Firing behavior of brain stem neurons during voluntary cancellation of the horizontal vestibuloocular reflex. II. Eye movement related neurons. *J. Neurophysiol* 1993; 70(2):844-56.
61. Cullen KE, McCrea RA. Firing behavior of brain stem neurons during voluntary cancellation of the

- horizontal vestibuloocular reflex. I. Secondary vestibular neurons. *Neurophysiol* 1993; 70(2):828-43.
62. McKinley PA, Peterson BW. Voluntary modulation of the vestibulo-ocular reflex in humans and its relation to smooth pursuit. *Exp Brain Res* 1985; 60: 454-64.
 63. Kornilova LN, et al. Pathogenesis of sensory disorders in microgravity. *Physiologist* 1991; 34:S36-39.
 64. André-Deshays C, Israel I, Charade O, Berthoz A, Popov K, Lipshits M. Gaze control in microgravity: I. Saccades, pursuit, eye-head coordination. *J Vest Res* 1993; 3:331-43.
 65. Young LR. Space and the vestibular system: what has been learned. *J Vestib Res Equilibrium & Orientation* 1993; 3:203-06.
 66. Rashbass C, Russell GFM. Action of a barbituate drug (Amylobarbitone Sodium) on the vestibulo-ocular reflex. *Brain* 1961; 84:329-35.
 67. Kowler E, Martins AJ, Pavel M. The effect of expectations on slow oculomotor control-IV. Anticipatory smooth eye movements depend on prior target motions. *Vision Res* 1984; 24:197-210.
 68. Robinson DA, Gordon JL, Gordon SE. A model of the smooth pursuit eye movement system. *Biol Cybern* 1986; 55:43-57.
 69. Blakemore C, Donaghy M. Coordination of head and eyes in the gaze changing behavior of cats. *J Physiol (Lond)* 1980; 300:317-35.
 70. Collewijn H, Conijn P, Tamminga EP. Eye-head coordination in man during the pursuit of moving targets. In: Lennerstrand G, Zee DS, Keller E, editors. *Functional basis of ocular motility disorders*. Oxford: Pergamon Press; 1982. p 369-78.
 71. Wist ER, Brandt T, Krafczak S. Oscillopsia and retinal slip. Evidence supporting a clinical test. *Brain* 1983; 106:153-68.
 72. Virre E, Tweed D, Milner K, Vilis T. A reexamination of the gain of the vestibuloocular reflex. *J Neurophysiol* 1986; 56:439-50.
 73. Hine T, Thorn F. Compensatory eye movements during active head rotation for near targets: effects of imagination, rapid head oscillation and vergence. *Vision Res* 1987; 27:1639-57.
 74. Collewijn H, Erkelens CJ, Steinman RM. Binocular coordination of human horizontal saccadic eye movements. *J Physiol (Lond)* 1988; 404:157-82.
 75. Leigh RJ, Zee DS. *The neurology of eye movements*. Philadelphia: F.A. Davis Co.; 1991.
 76. Guitton D, Volle M. Gaze control in humans; eye-head coordination during orienting movements to targets within and beyond the oculomotor range. *J Neurophysiol* 1989; 58:427-59.
 77. Zangemeister WH, Stark L. Gaze latency; variable interactions of head and eye latency. *Exp Neurol* 1982; 75:389-406.

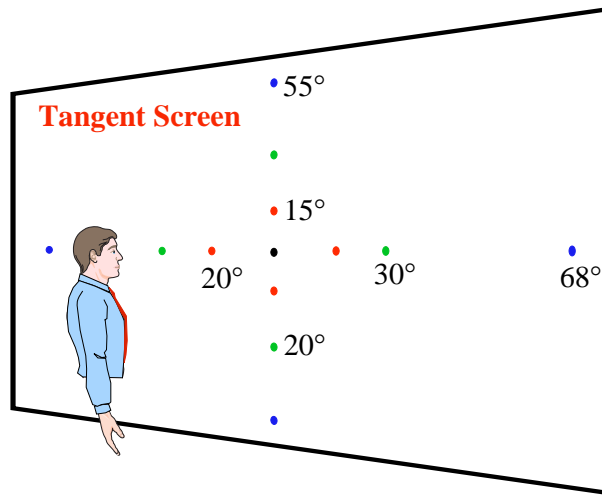


Figure 5.3-1. Representation of target location on tangent screen.

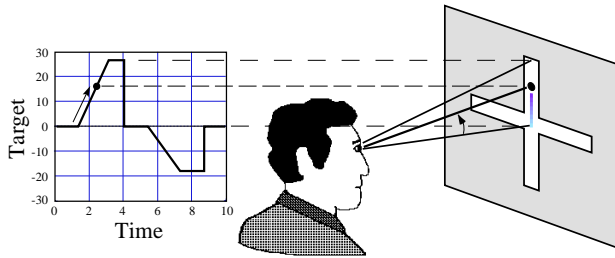


Figure 5.3-2. Unpredictable pursuit tracking: ramp stimulus.

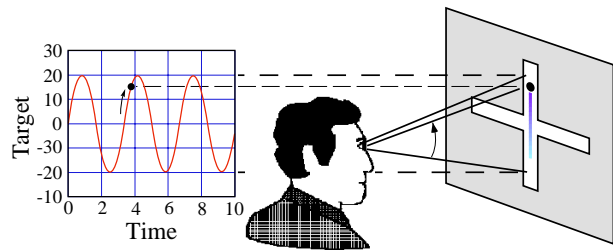


Figure 5.3-3. Predictable smooth pursuit: sinusoidal stimulus.

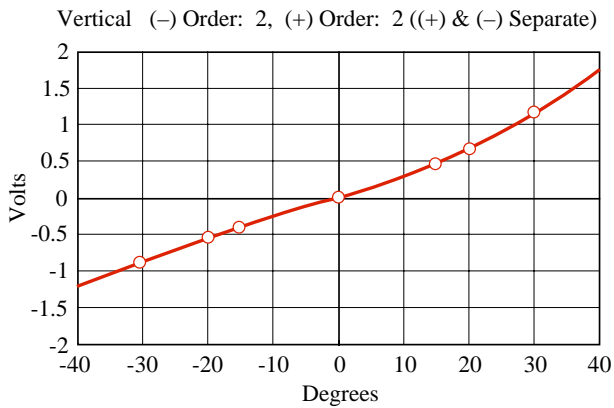


Figure 5.3-4a. Vertical eye calibration.

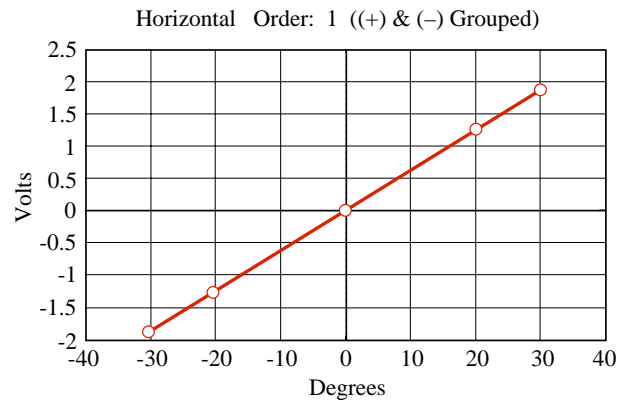


Figure 5.3-4b. Horizontal eye calibration.

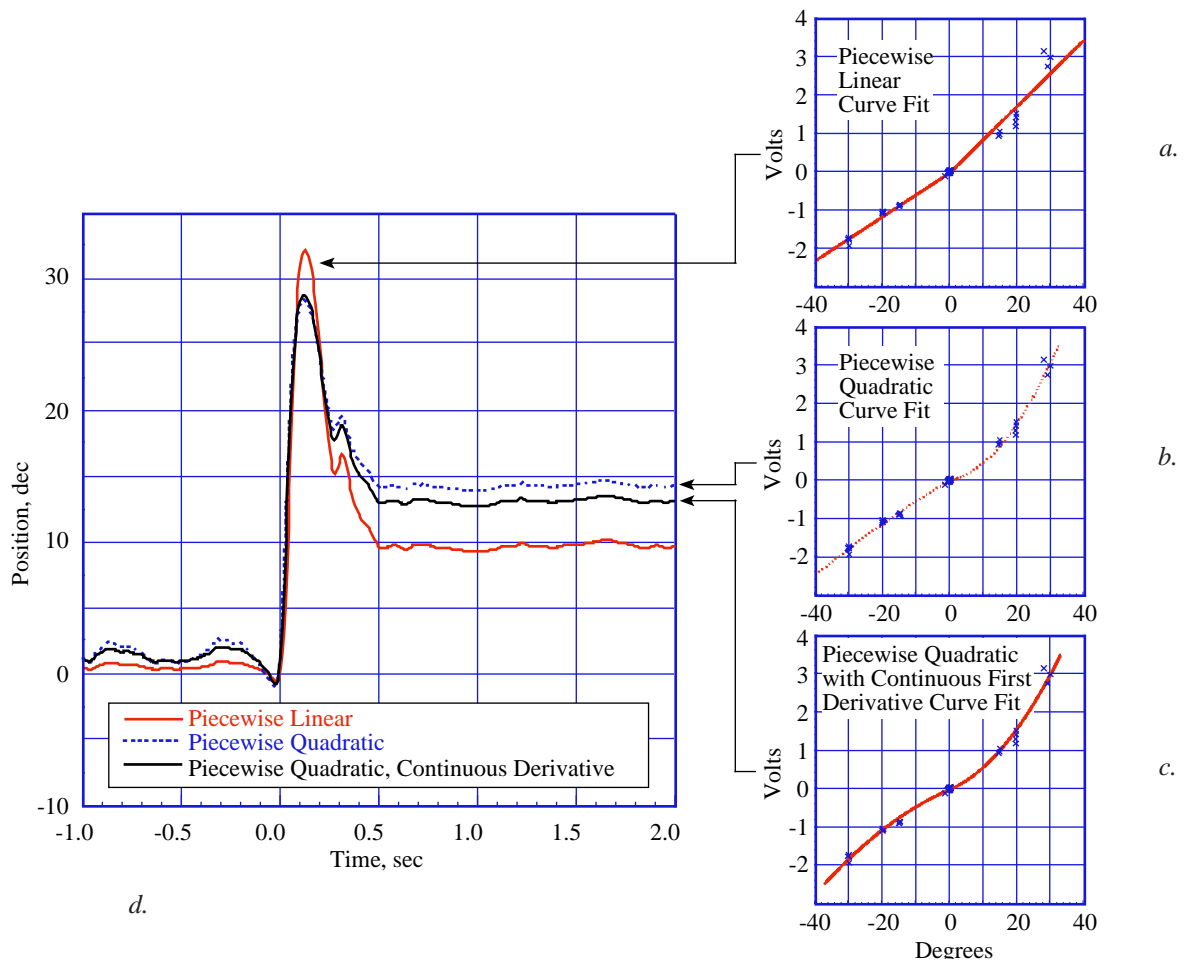


Figure 5.3-5. Various calibration curves applied to a vertical target acquisition eye movement response.

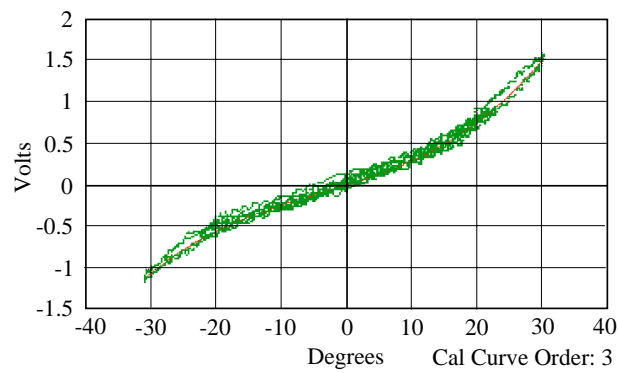
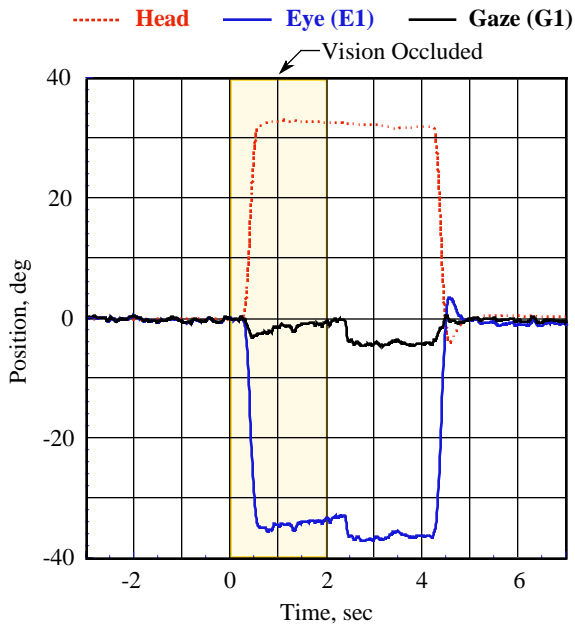


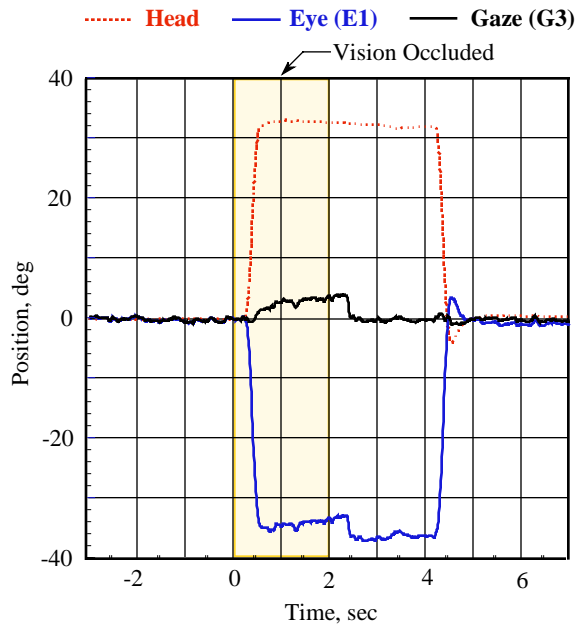
Figure 5.3-6. Dynamic, fixed-gaze eye calibration curve – vertical.

Simple Calculation of Gaze ($G = E + H$):
 Gaze Referenced to Displaced Location of Eye in Space



a.

Geometry of Eye Eccentricity Considered in Calculation of Gaze:
 Gaze Referenced to Primary Eye Position with Head at Zero



b.

Figure 5.3-7. Geometrical gaze correction.

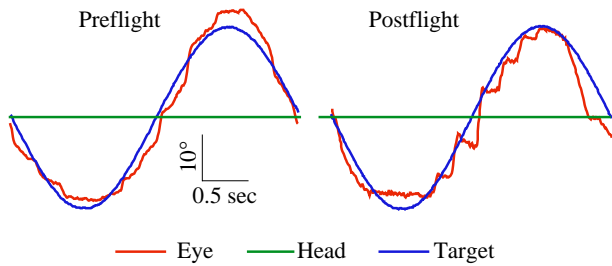
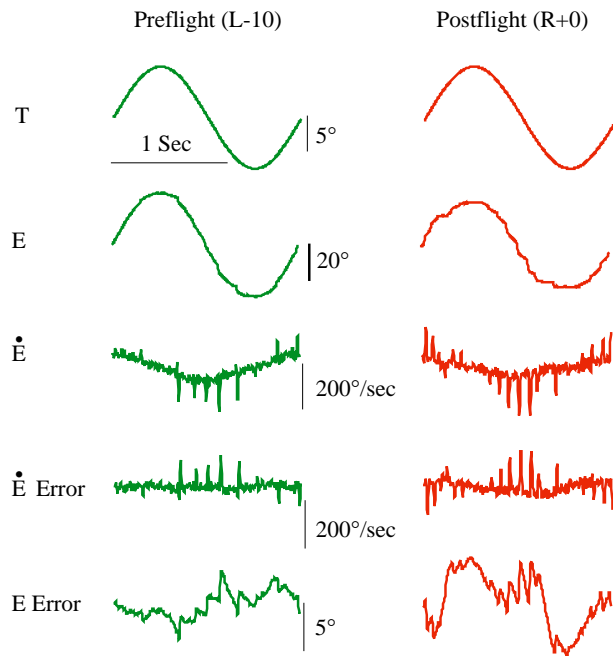


Figure 5.3-8. Vertical smooth pursuit: eyes only.



T = Target Wave Form
 E = Horizontal Eyes
 \dot{E} = Eye Velocity
 \dot{E} Error = Eye Error Velocity
 E Error = Eye Error Position

Figure 5.3-9. Horizontal smooth pursuit: eyes only.

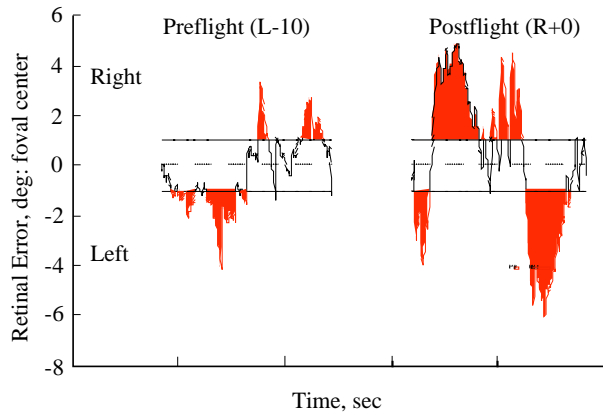


Figure 5.3-10. Cumulative time foveation is off target.

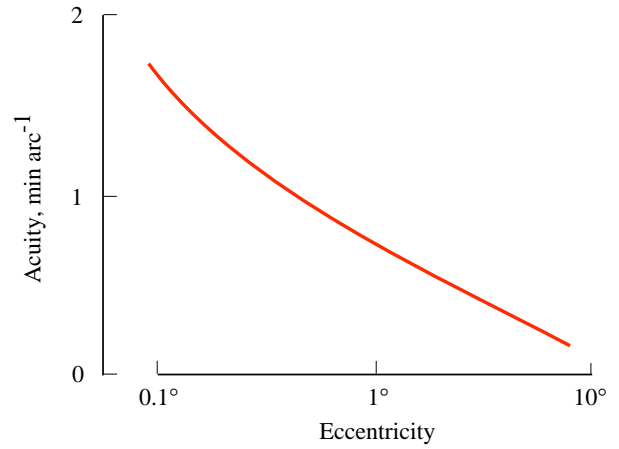


Figure 5.3-11. Loss of acuity with target displacement from foveal center.

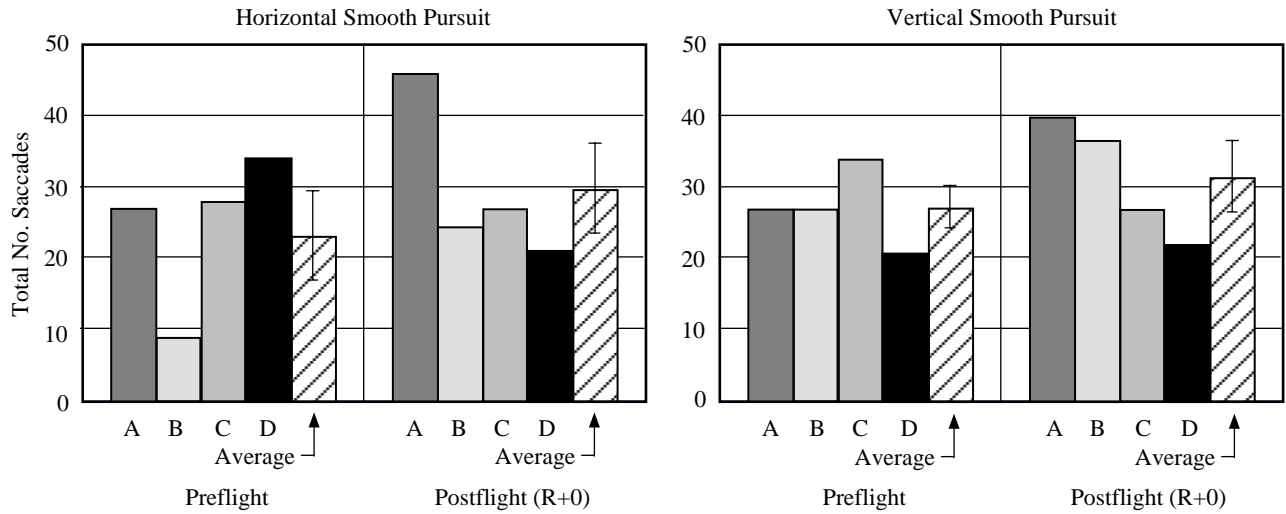


Figure 5.3-12. Total Number of Saccades.

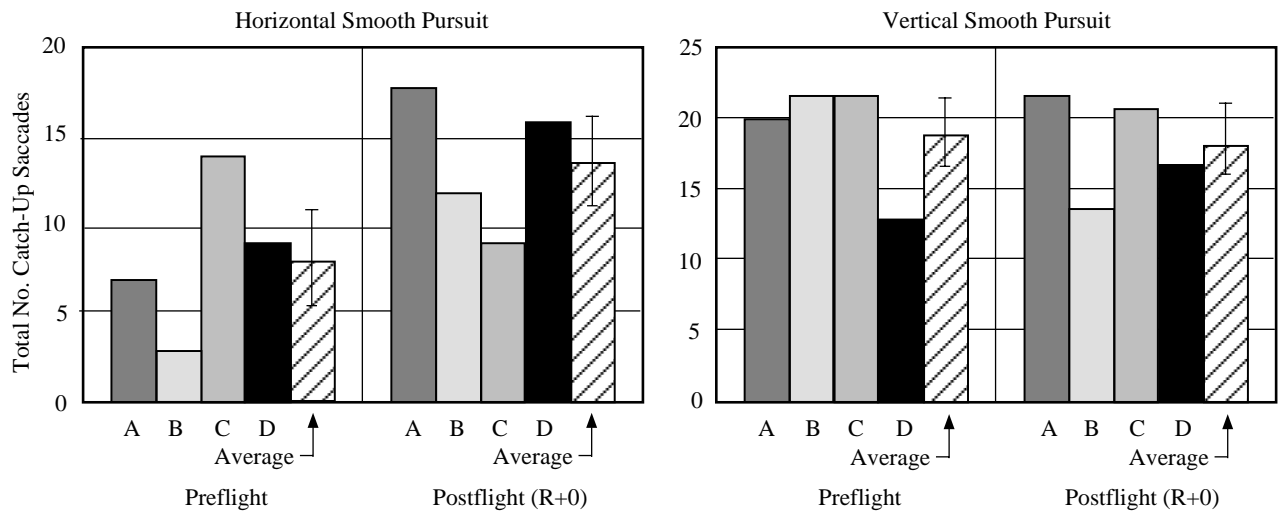


Figure 5.3-13. Total Catch-up Saccades.

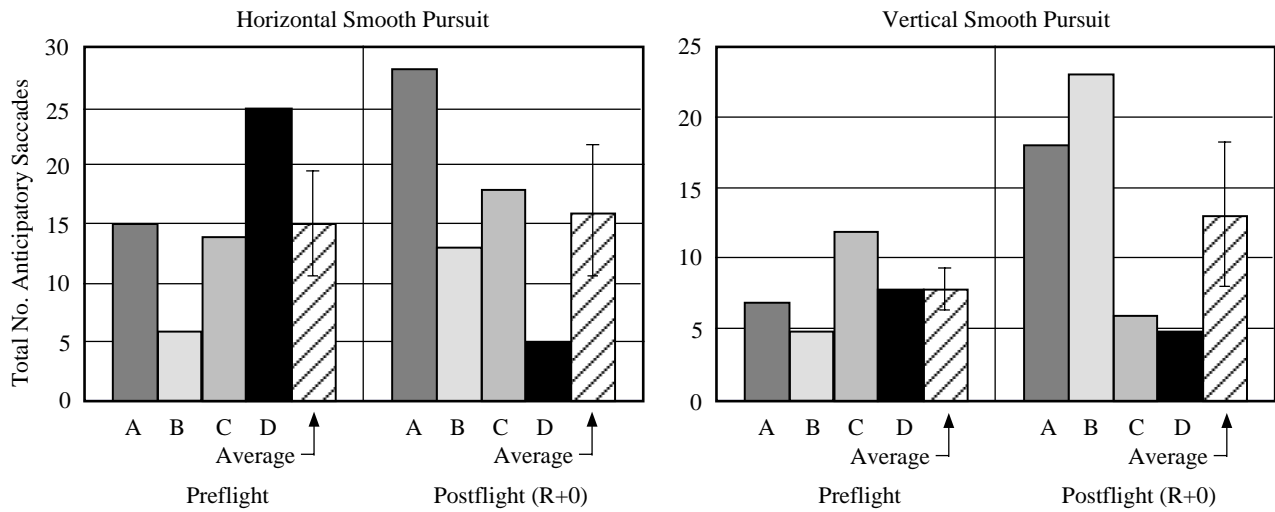


Figure 5.3-14. Total Anticipatory Saccades.

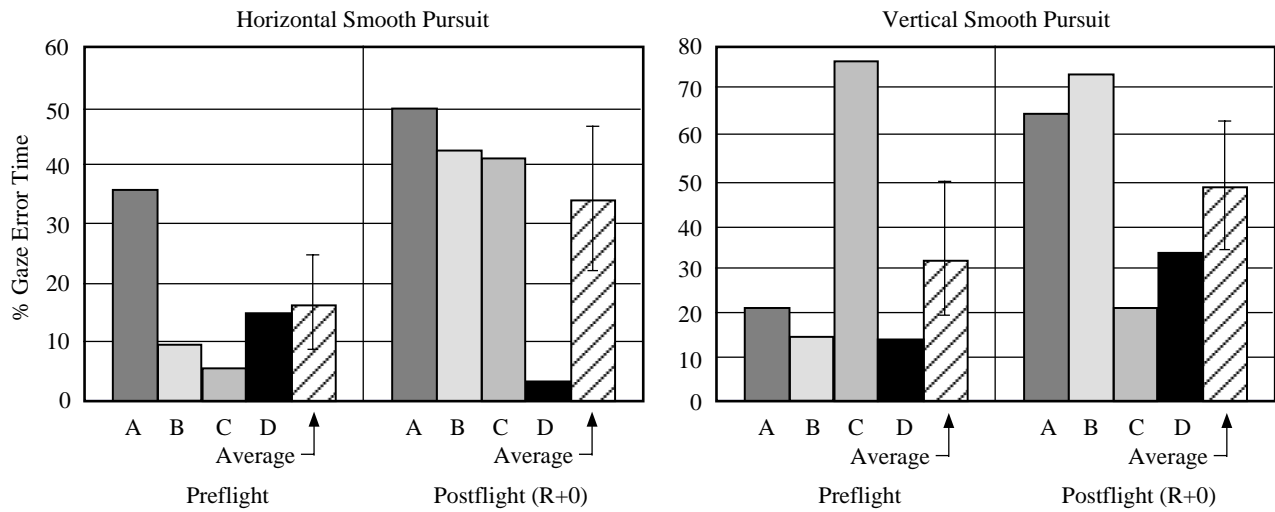


Figure 5.3-15. Cumulative gaze error time (%).

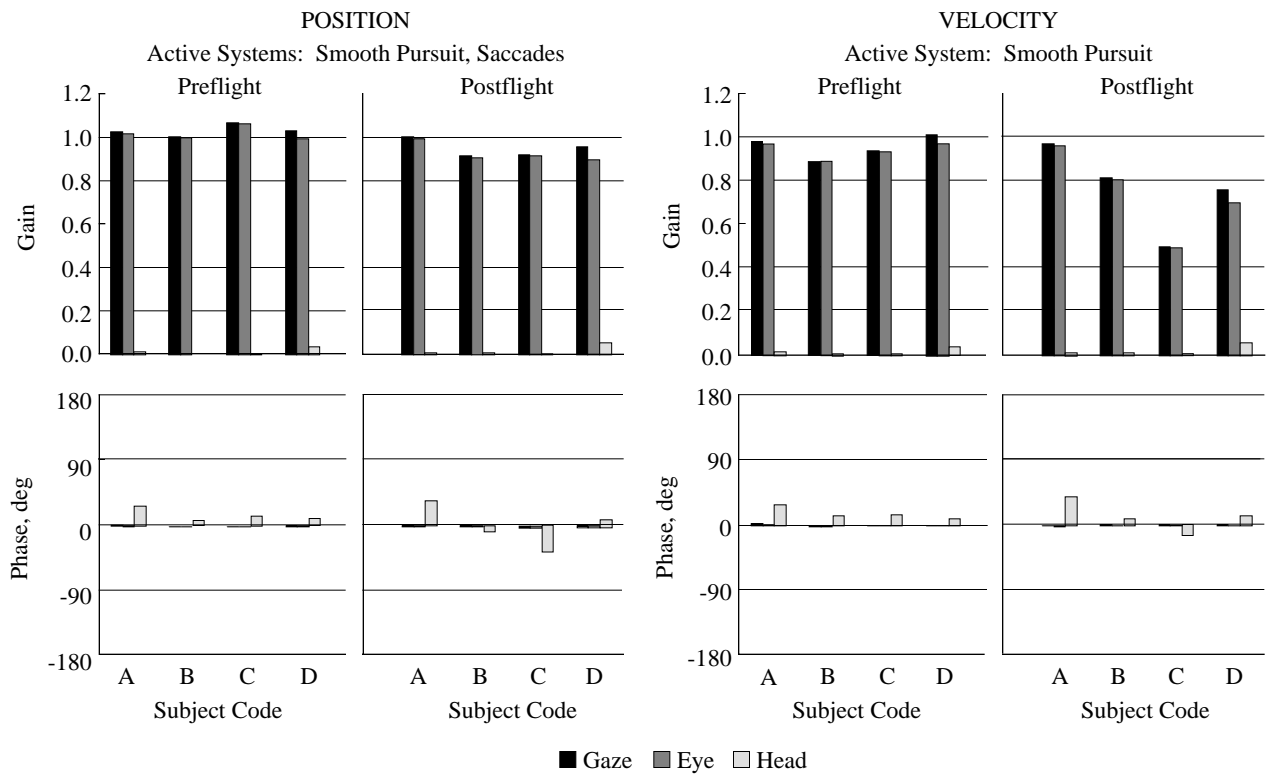
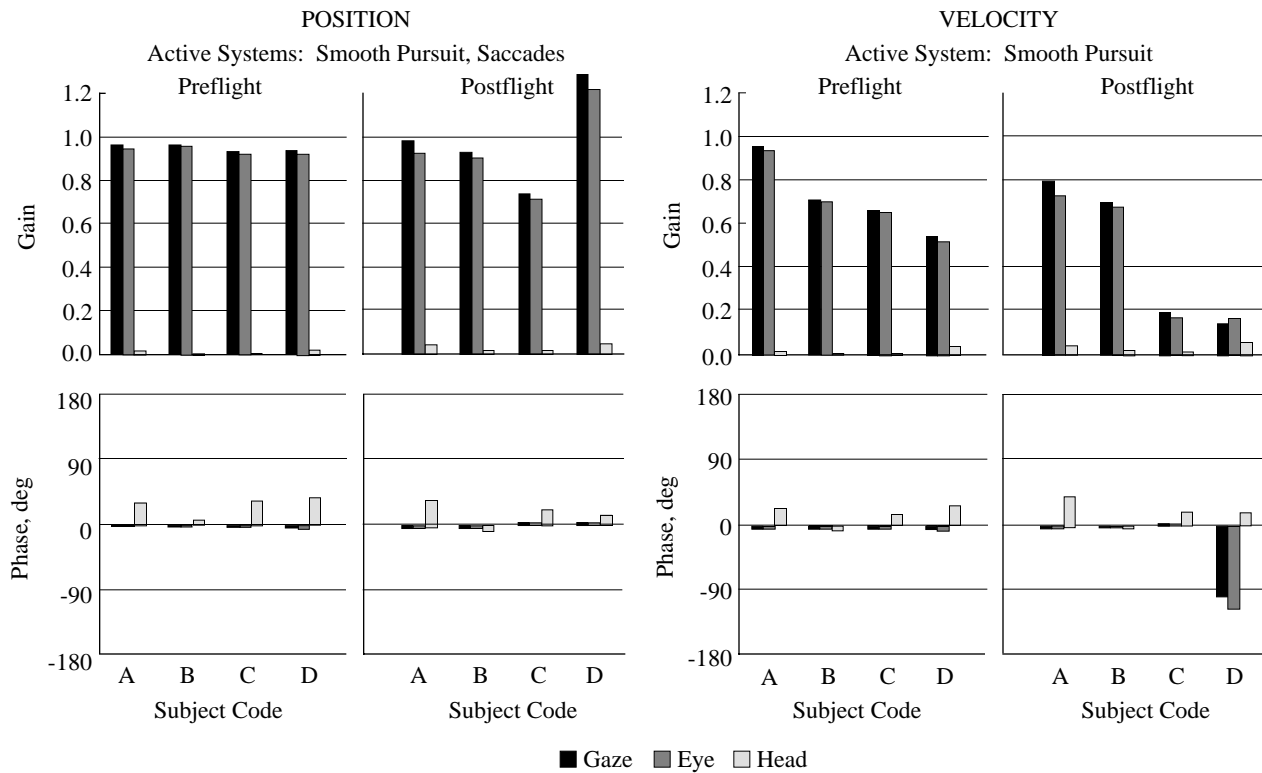


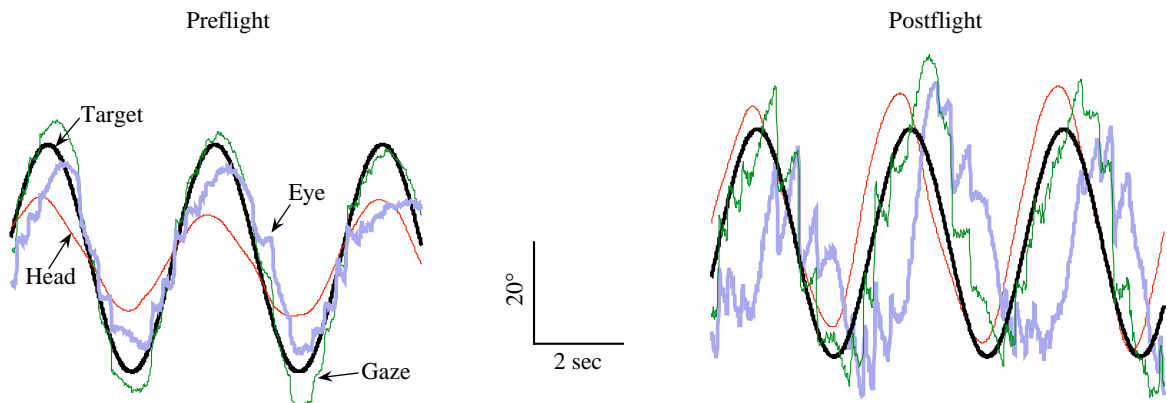
Figure 5.3-16. Horizontal – smooth pursuit (eyes only).



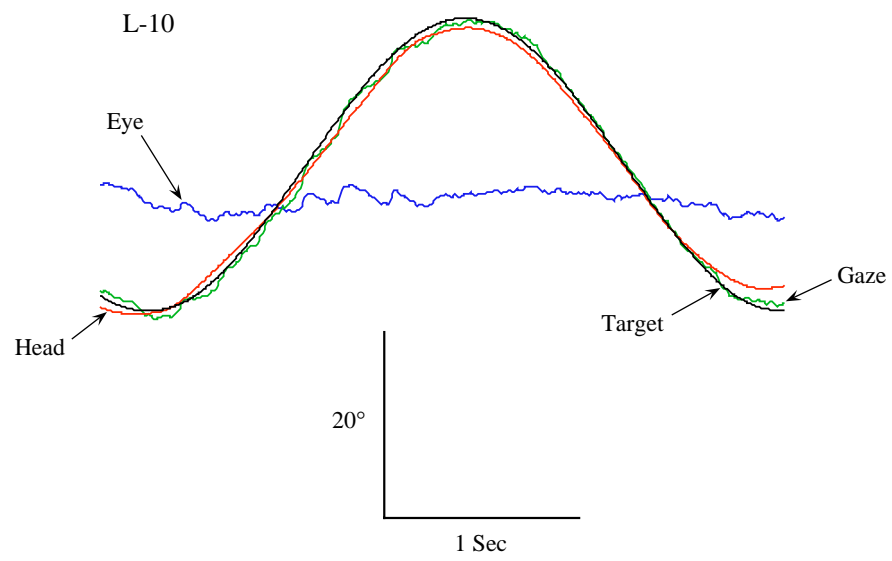
a.

b.

Figure 5.3-17. Vertical – smooth pursuit (eyes only).



a.



b.

Figure 5.3-18. Vertical pursuit tracking with head and eyes.

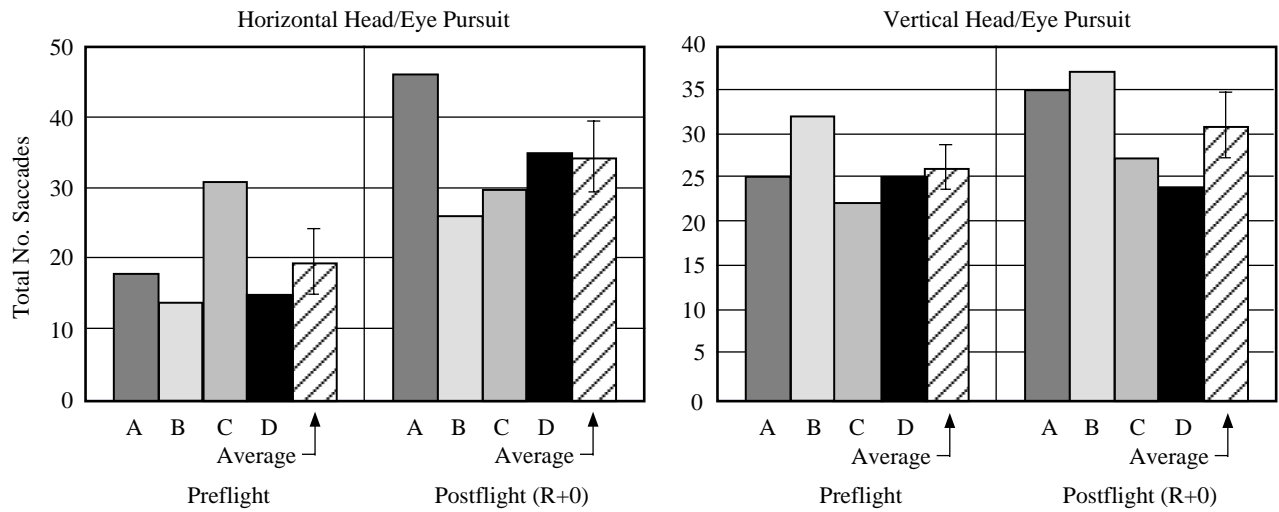


Figure 5.3-19. Total Number of Saccades.

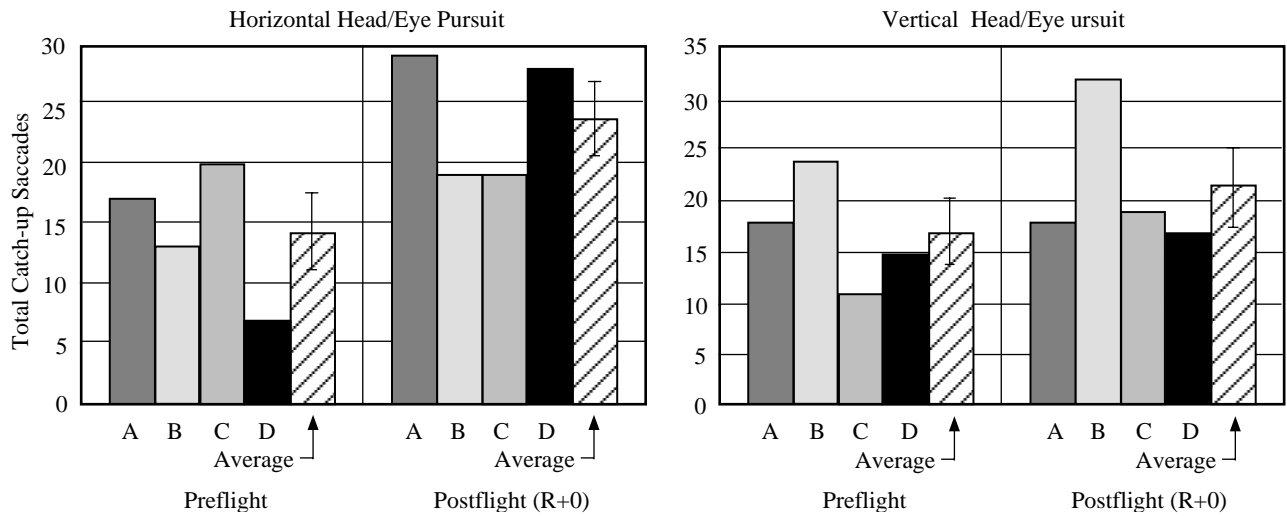


Figure 5.3-20. Total Catch-Up Saccades.

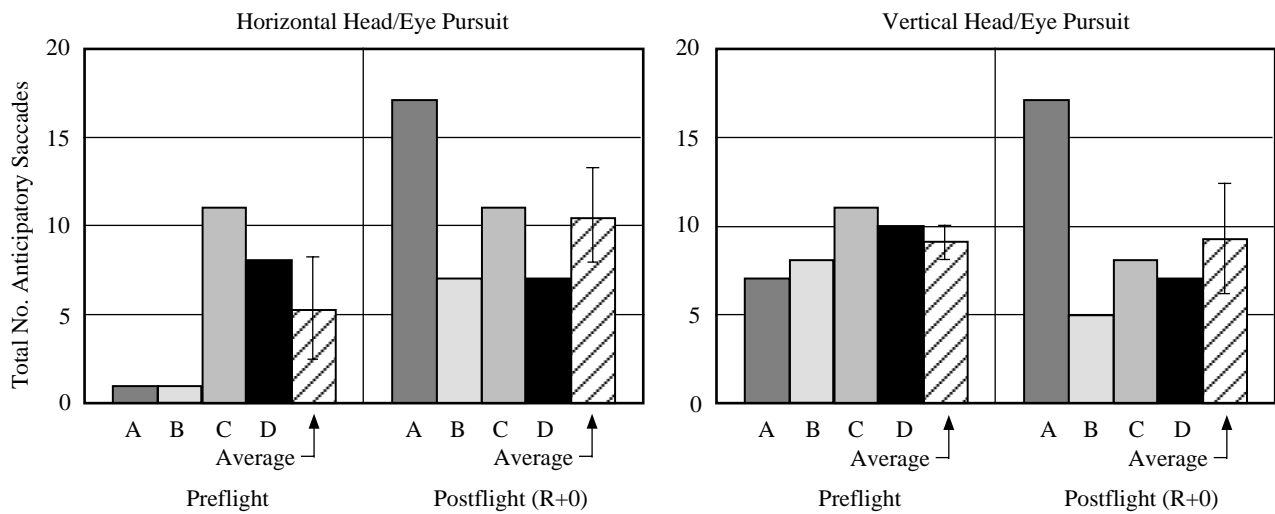


Figure 5.3-21. Total Anticipatory Saccades.

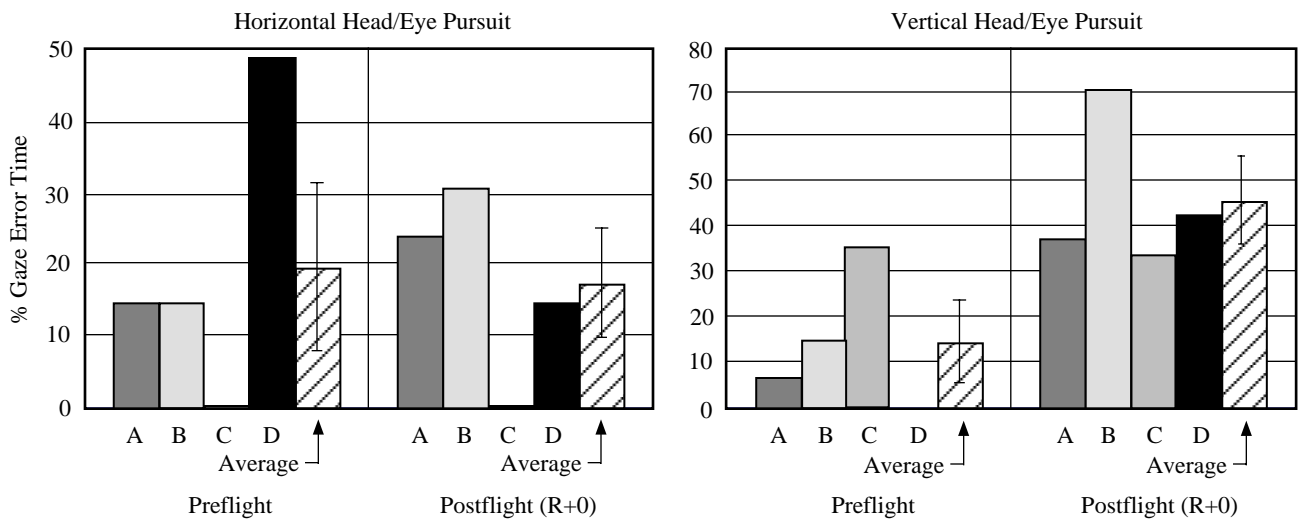


Figure 5.3-22. Cumulative gaze error time (%).

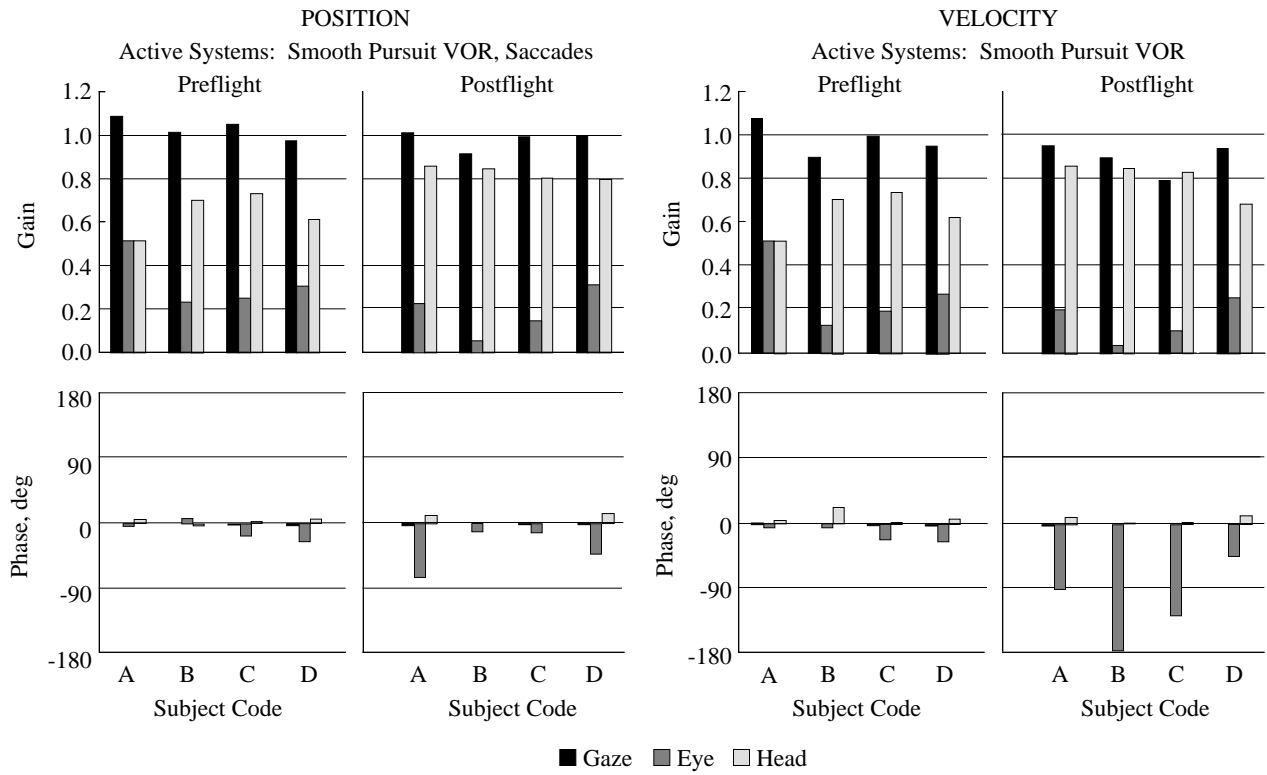


Figure 5.3-23. Horizontal – eye-head tracking.

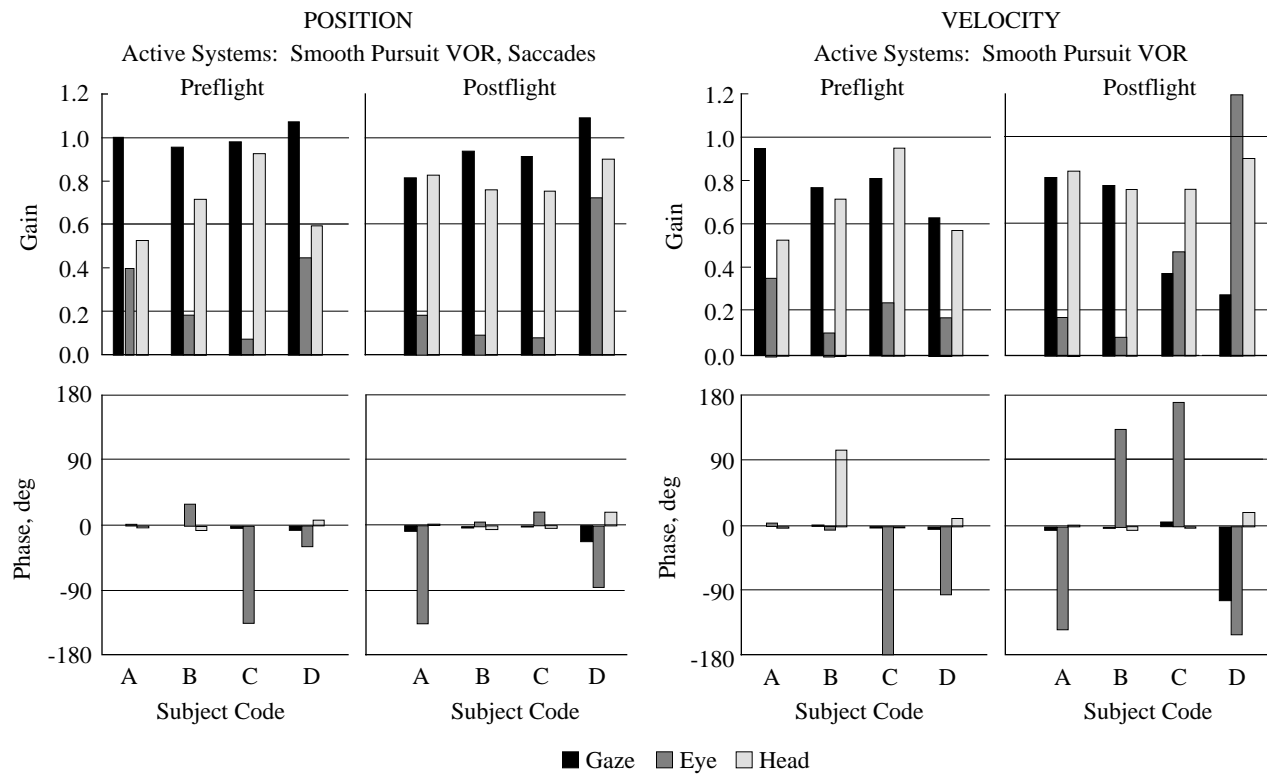


Figure 5.3-24. Vertical – eye-head tracking.

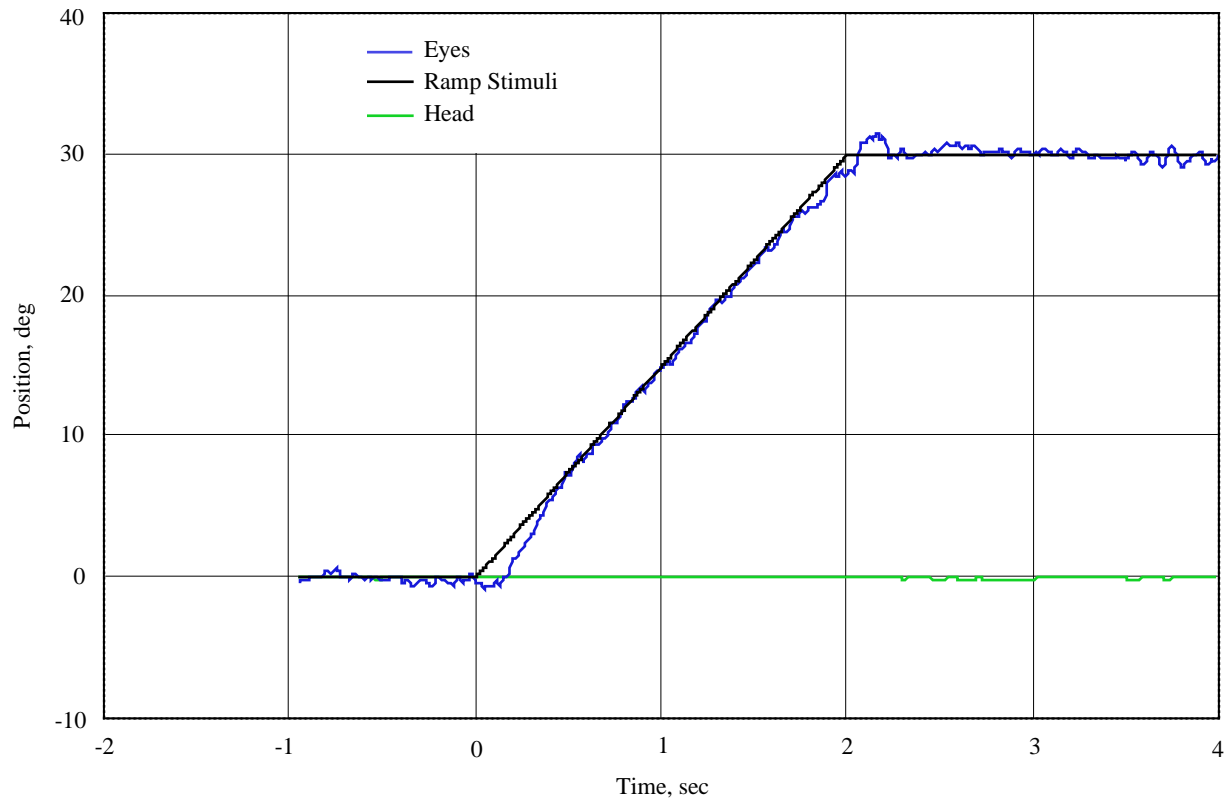


Figure 5.3-25. L-10 Unpredictable pursuit tracking: Low velocity (15°/sec) ramp tracking with eye ramp moving rightward.

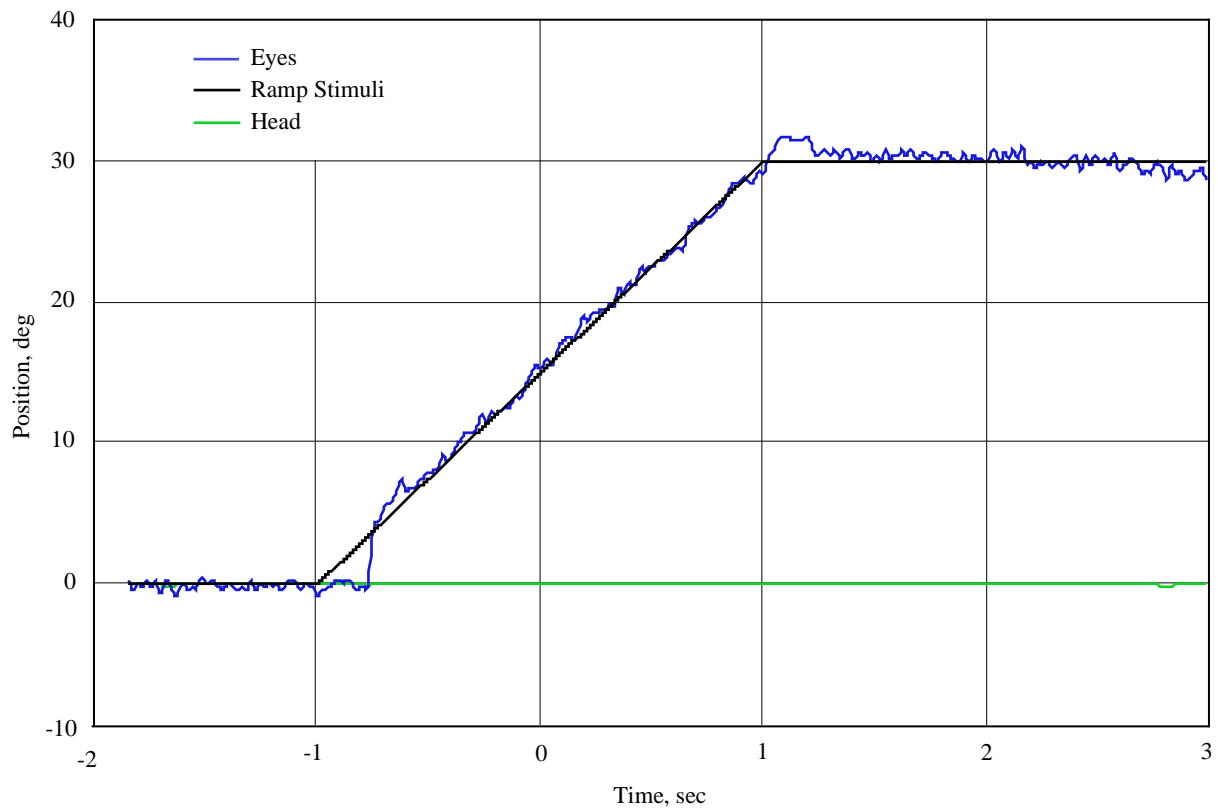


Figure 5.3-26. R+0 Unpredictable pursuit tracking: Low velocity (15°/sec) ramp tracking with eye ramp moving rightward.

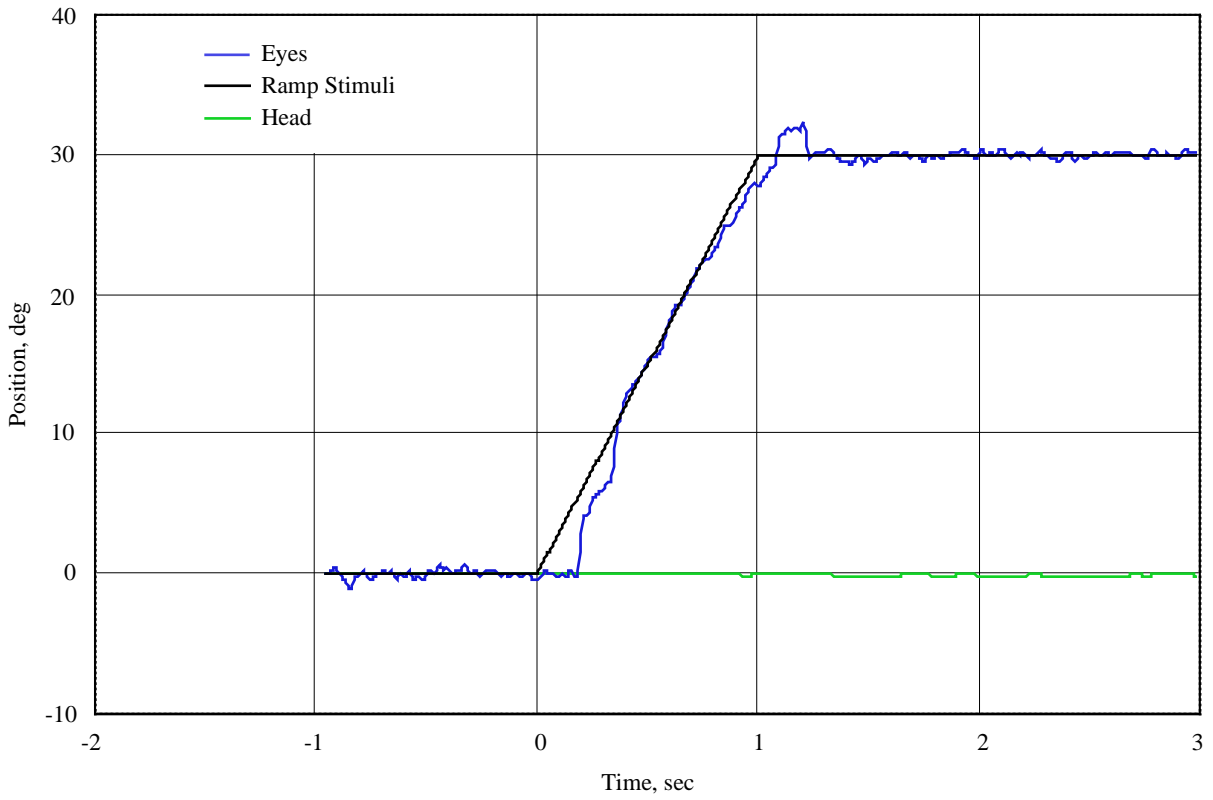


Figure 5.3-27. L-10 Unpredictable pursuit tracking: Low velocity (30°/sec) ramp tracking with eye ramp moving rightward.

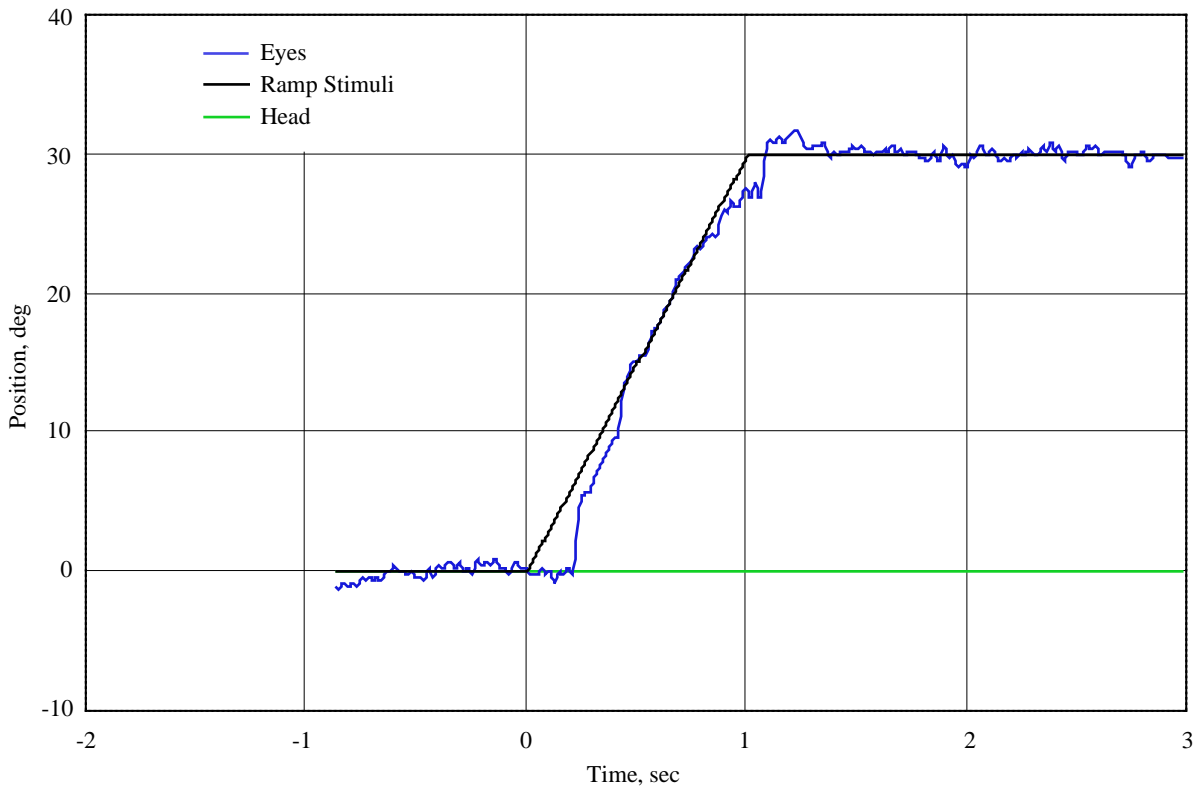


Figure 5.3-28. R+0 Unpredictable pursuit tracking: Low velocity (30°/sec) ramp tracking with eye ramp moving rightward.

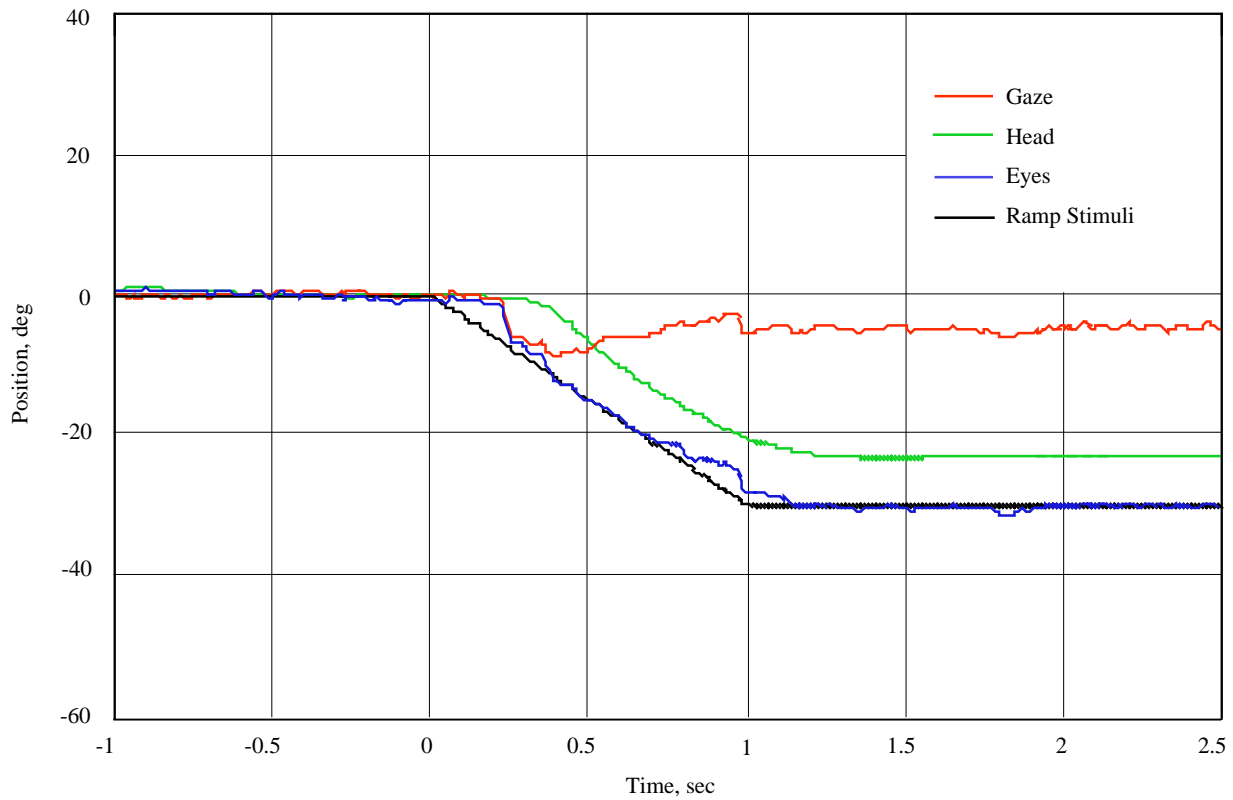


Figure 5.3-29. L120 Unpredictable pursuit tracking: High velocity ($30^\circ/\text{sec}$) ramp tracking with both head and eye, with a ramp moving leftward.

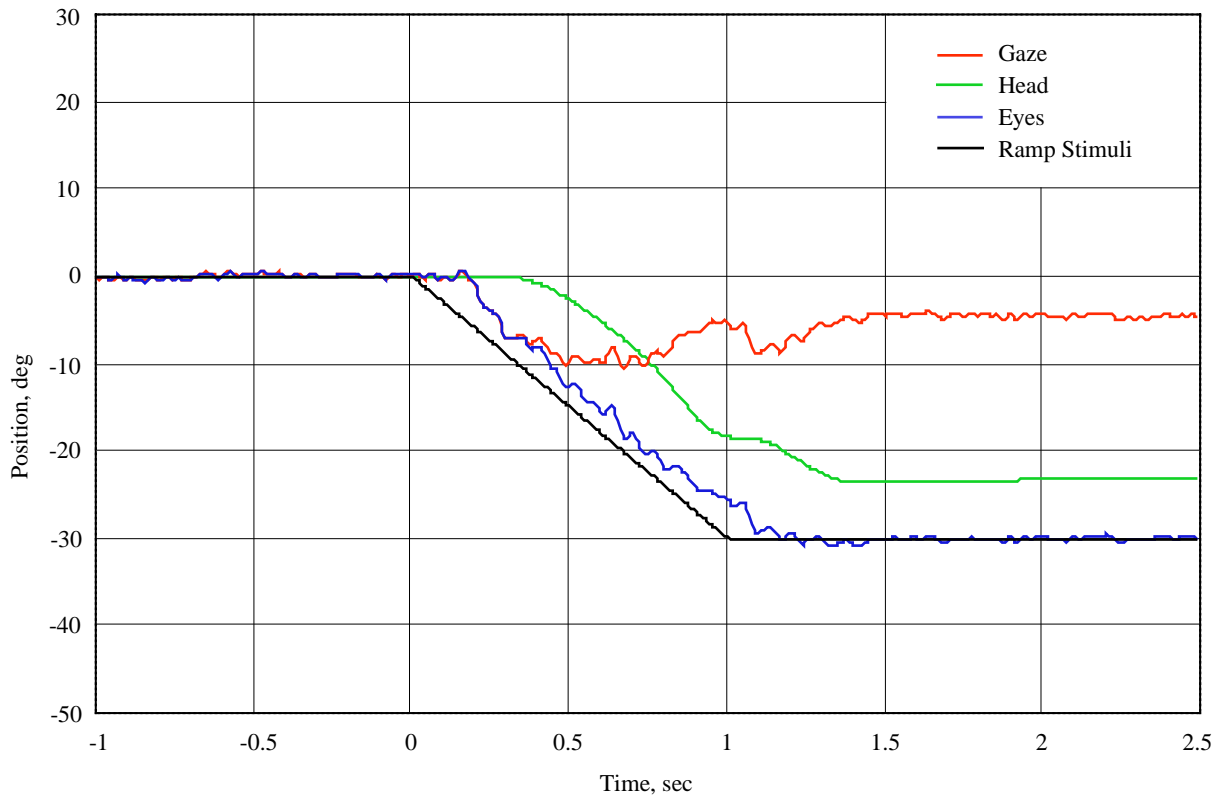


Figure 5.3-30. R+0 Unpredictable pursuit tracking: High velocity ($30^\circ/\text{sec}$) ramp tracking with both head and eye, with a ramp moving leftward.

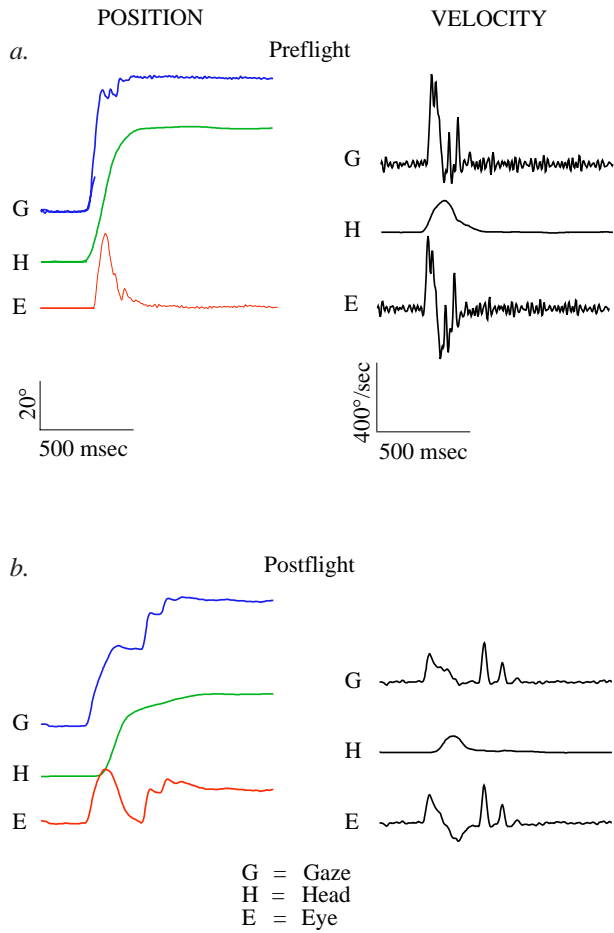


Figure 5.3-31. Pre and postflight target acquisition in vertical plane.

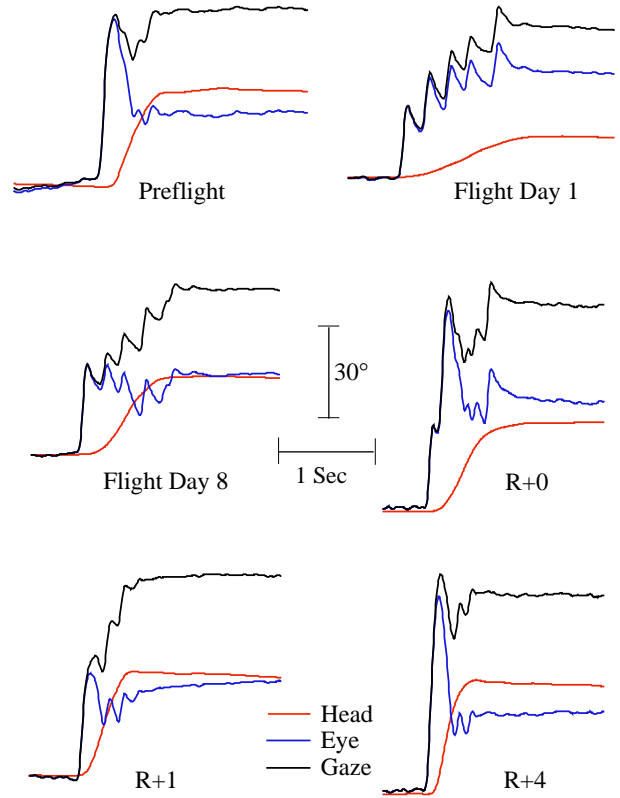


Figure 5.3-32. Upward target acquisition nearing the EOM (+50°).

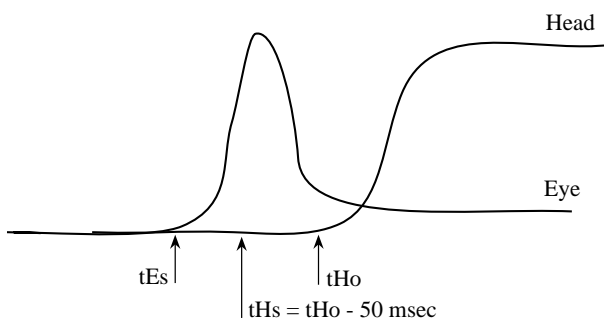


Figure 5.3-33. An illustration of how delays of head and eye movements are designated for quantification of the five different Stark types.

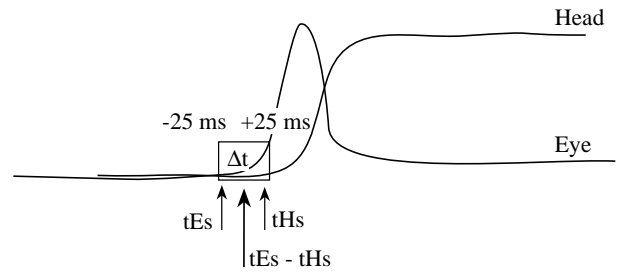


Figure 5.3-34. Stark type I $tEs - tHs > \Delta t$ and $< +\Delta t$.

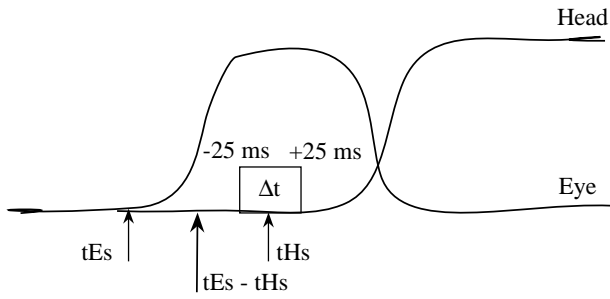


Figure 5.3-35. Stark type II $tEs - tHs < \Delta t$.

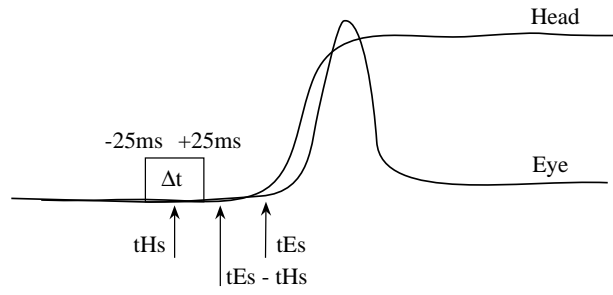


Figure 5.3-36. Stark type IIIa $tEs - tHs > + \Delta t$ and < 150 msec.

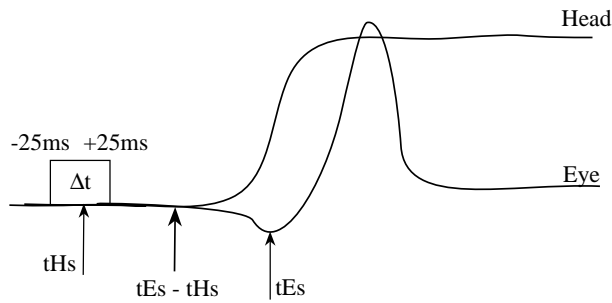


Figure 5.3-37. Stark type IIIb $tEs - tHs > 150$ msec and < 500 msec.

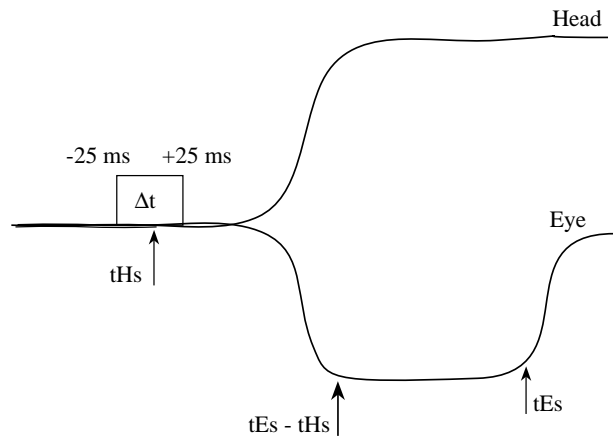


Figure 5.3-38. Stark type IV $tEs - tHs > 500$ msec.

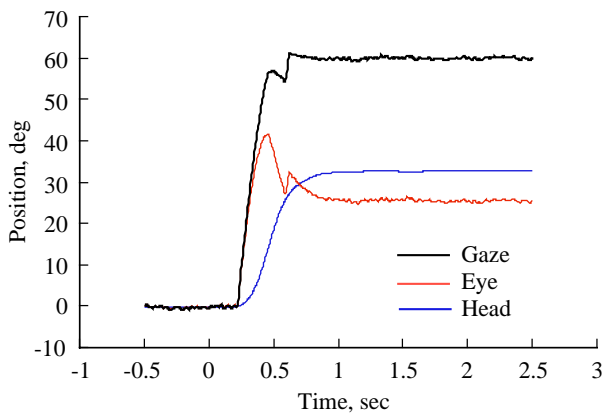


Figure 5.3-39. Preflight acquisition of target beyond the EOM.

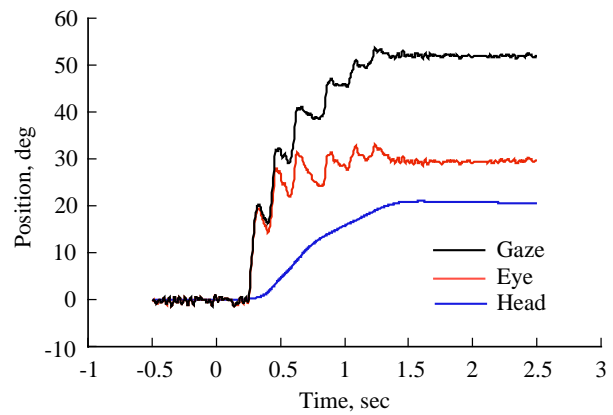


Figure 5.3-40. Postflight acquisition of a target beyond the EOM.

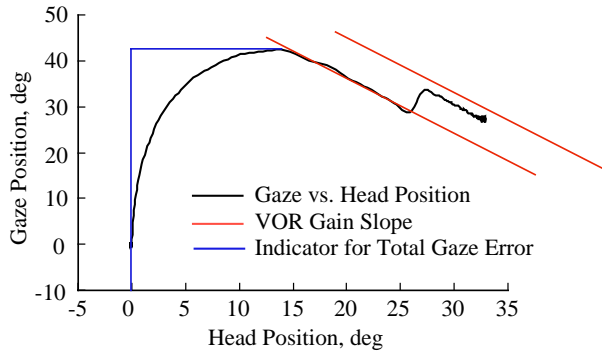


Figure 5.3-41. Gaze plane showing preflight total gaze error and VOR gain.

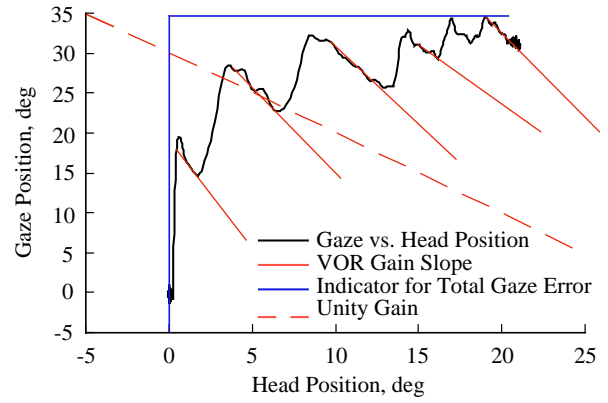


Figure 5.3-42. Gaze plane showing postflight total gaze error and VOR gain.

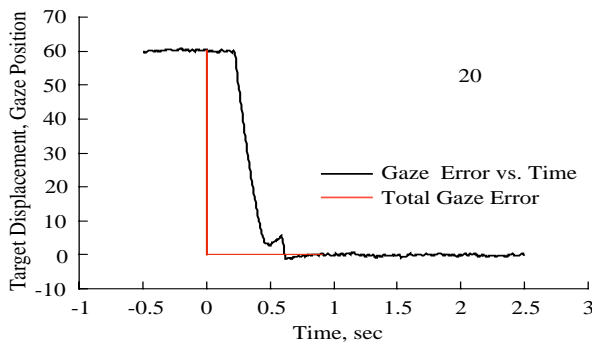


Figure 5.3-43. Preflight gaze error.

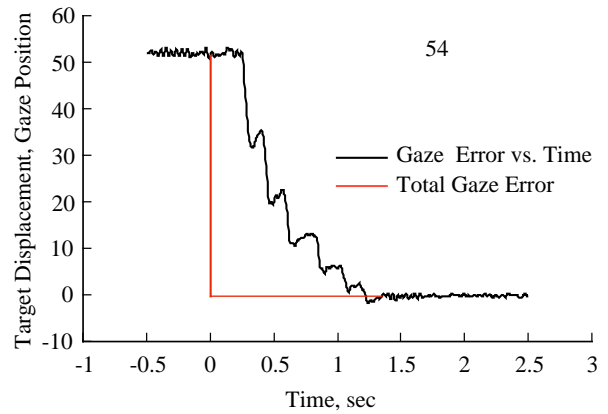


Figure 5.3-44. Postflight gaze error.

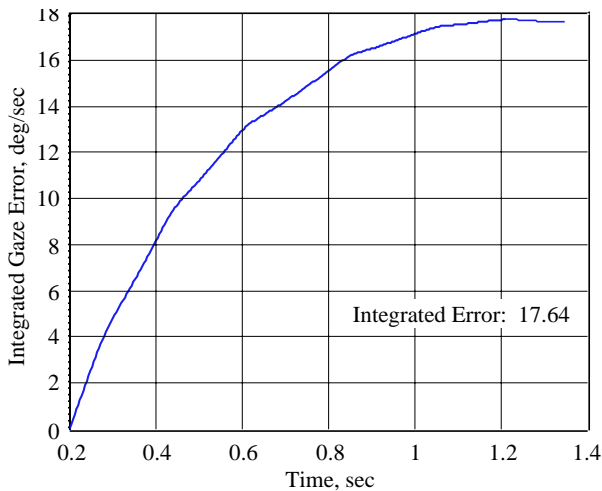


Figure 5.3-45. Integrated gaze error over time.

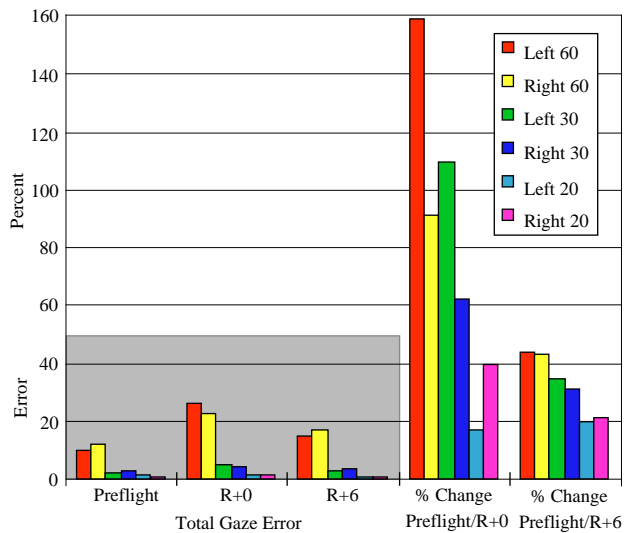


Figure 5.3-46. Changes in gaze error during flight for target displacement and recovery following flight.

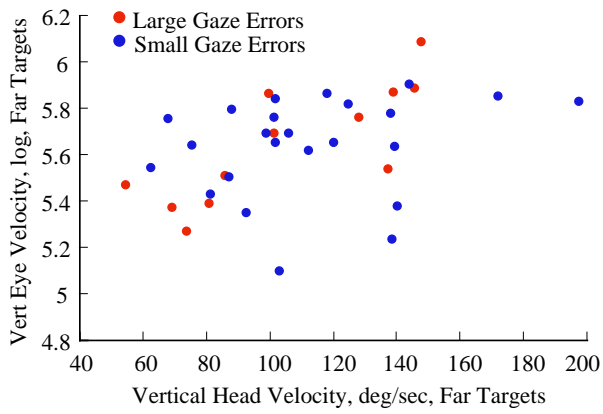


Figure 5.3-47. Postflight performance based on preflight gaze error.

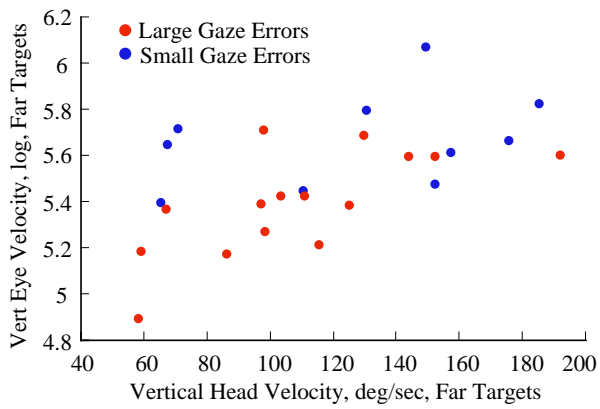


Figure 5.3-48. Postflight performance based on inflight gaze error.

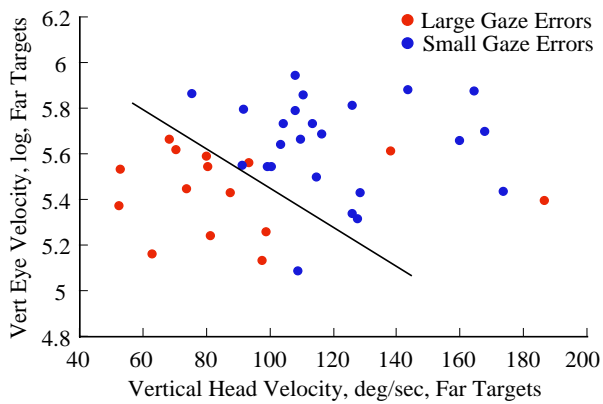


Figure 5.3-49. Postflight performance based on gaze error.

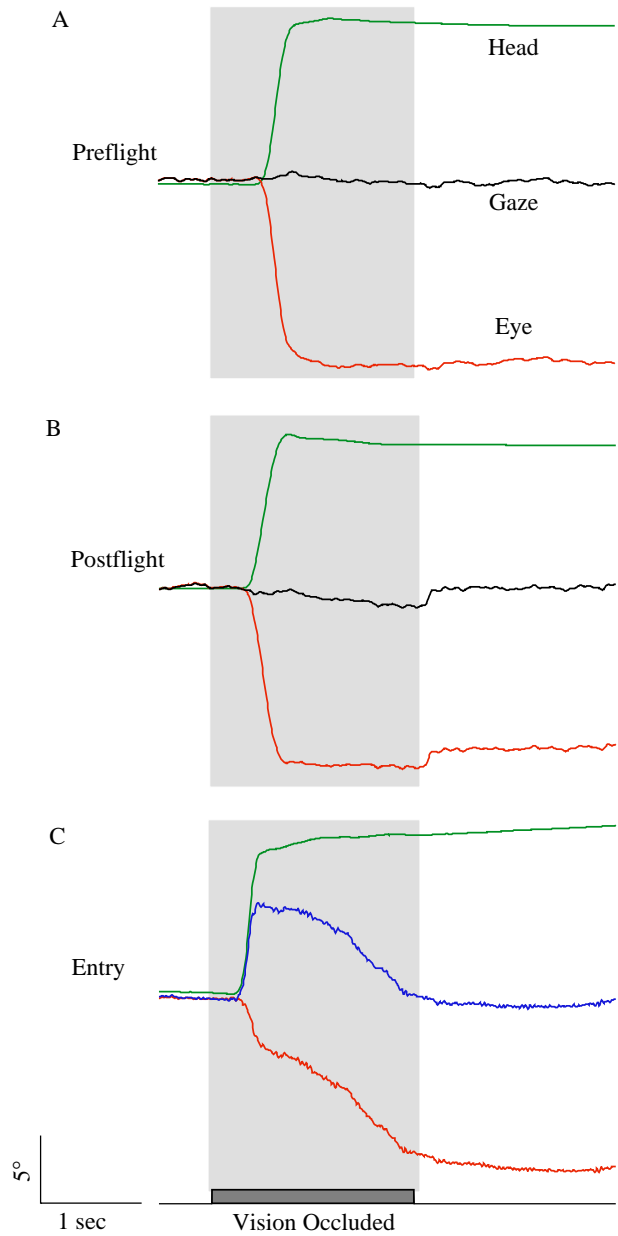


Figure 5.3-50. Gaze stabilization as a function of flight phase.

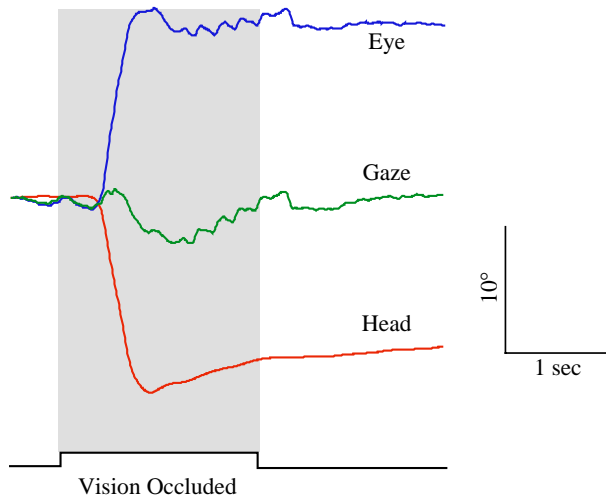


Figure 5.3-51. Postflight gaze stabilization with associated saccadic activity.

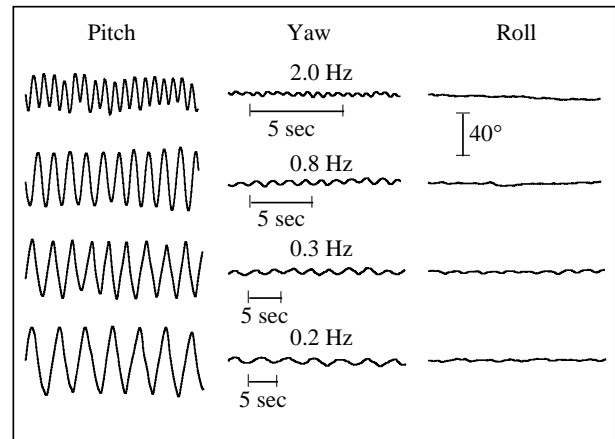


Figure 5.3-52. Sinusoidal head shakes: peak-to-peak displacements with vision during voluntary head shakes in the vertical plane.

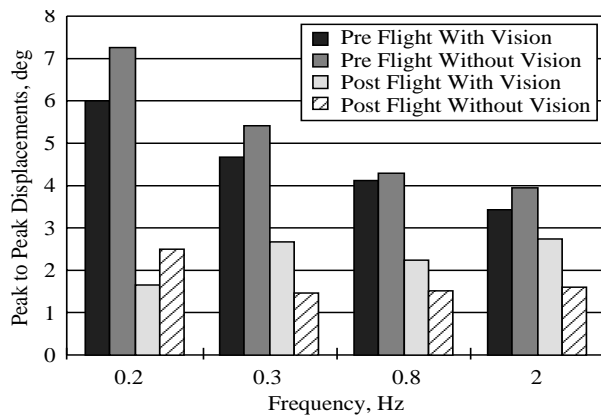


Figure 5.3-53. Displacement in the yaw plane during pitch head shakes: effects of flight phase and vision.

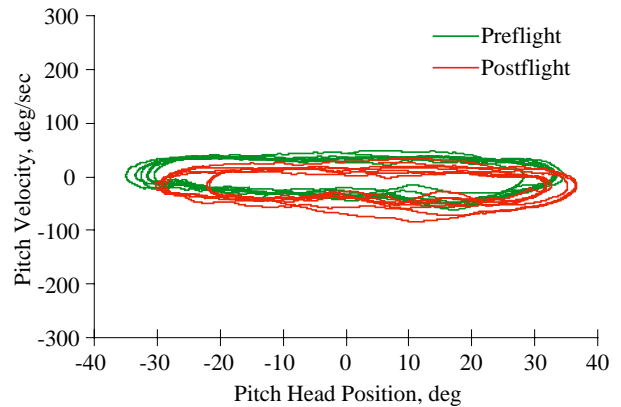


Figure 5.3-54. Phase plane for 0.2 Hz vertical head shake with vision.

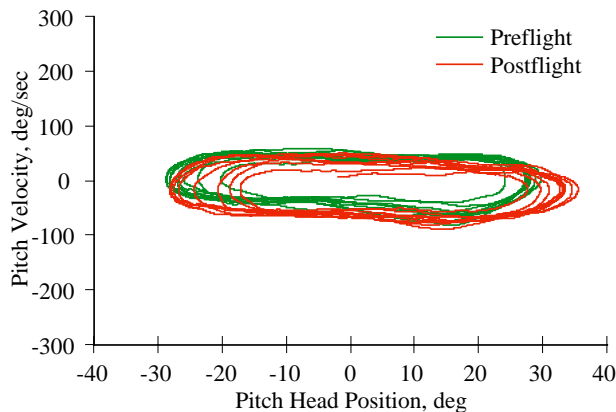


Figure 5.3-55. Phase plane for 0.3 Hz vertical head shake with vision.

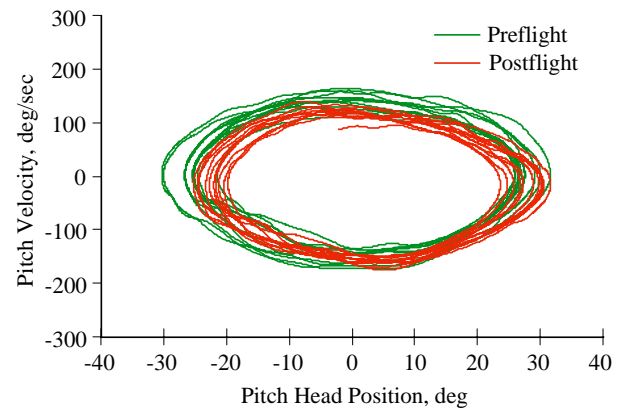


Figure 5.3-56. Phase plane for 0.8 Hz vertical head shake with vision.

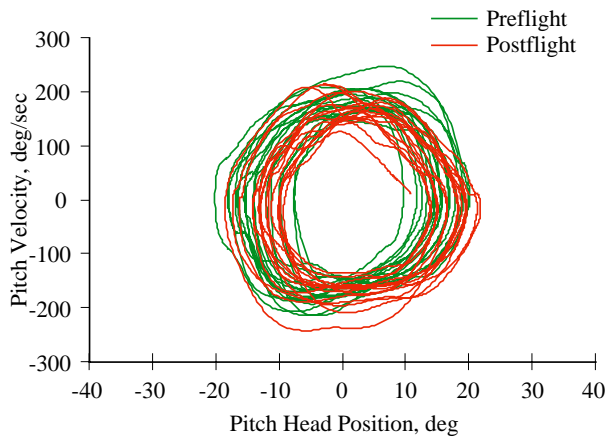


Figure 5.3-57. Phase plane for 2.0 Hz vertical head shake with vision.

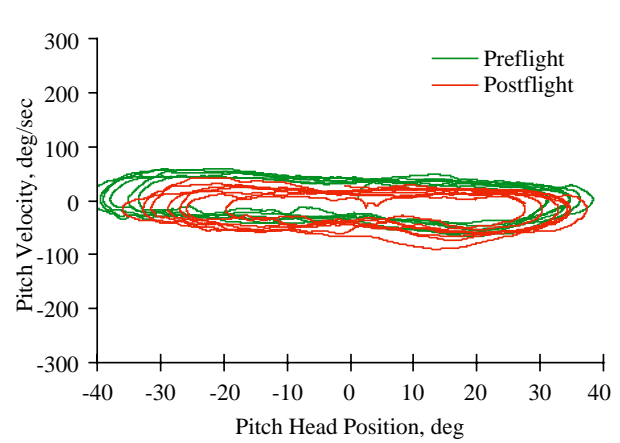


Figure 5.3-58. Phase plane for 0.2 Hz vertical head shake without vision.

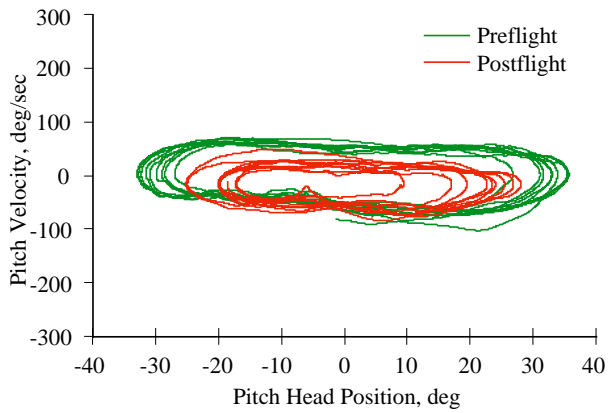


Figure 5.3-59. Phase plane for 0.3 Hz vertical head shake without vision.

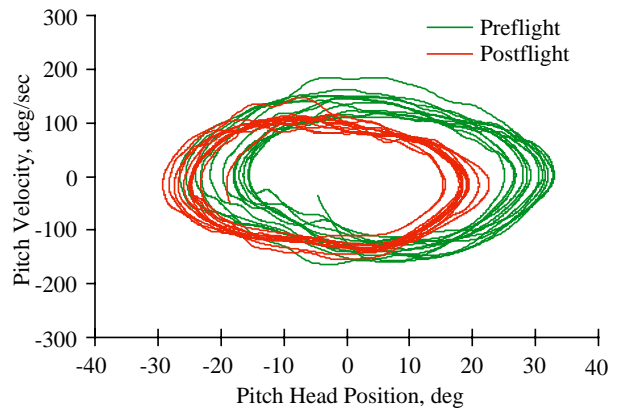


Figure 5.3-60. Phase plane for 0.8 Hz vertical head shake without vision.

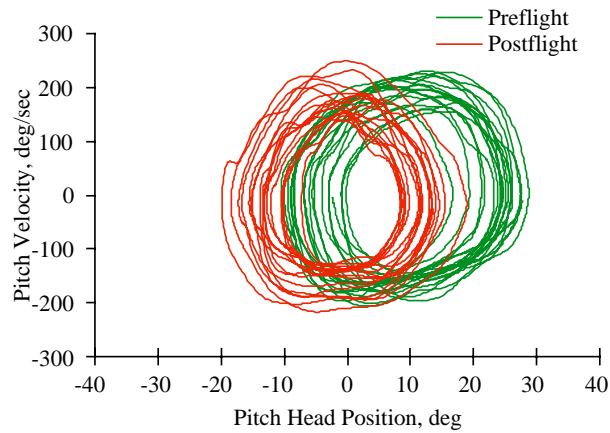


Figure 5.3-61. Phase plane for 2.0 Hz vertical head shake without vision.

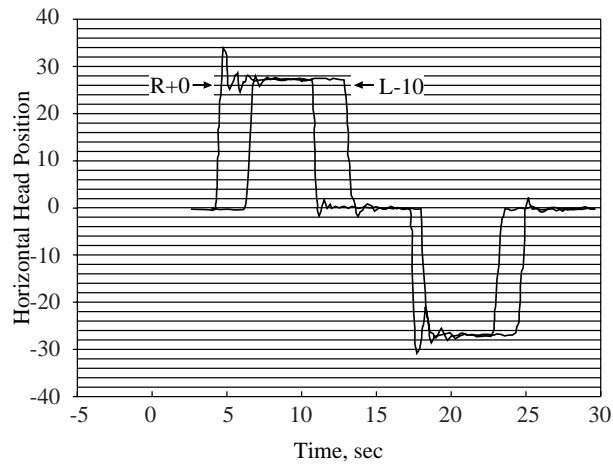


Figure 5.3-62. Horizontal head calibration, velocity:
subject 1.

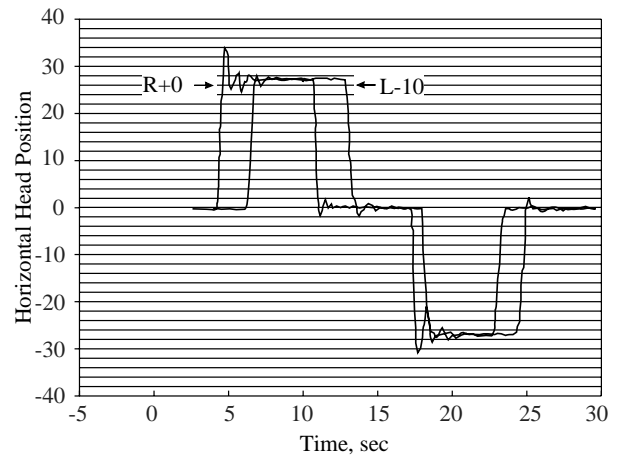


Figure 5.3-63. Horizontal head calibration position:
subject 2.

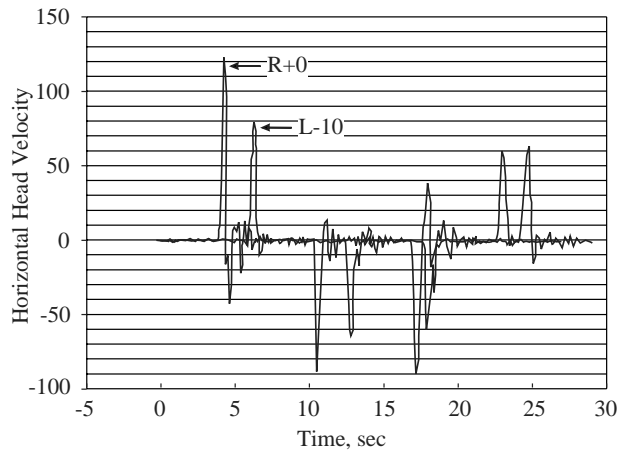


Figure 5.3-64. Horizontal head calibration velocity:
subject 1.

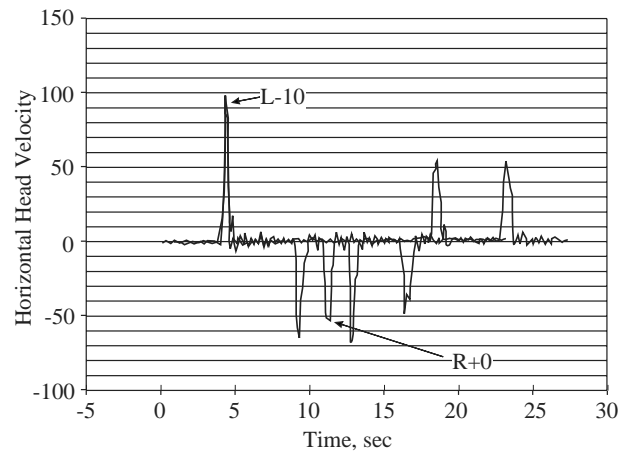


Figure 5.3-65. Horizontal head calibration velocity:
subject 2.